



Characterization of cellular toxicity induced by sub-lethal inorganic mercury in the marine microalgae *Chlorococcum dorsiventrale* isolated from a metal-polluted coastal site

Jihen Thabet^{a,b}, Jihen Elleuch^c, Flor Martínez^b, Slim Abdelkafi^c, Luis Eduardo Hernández^{b,*}, Imen Fendri^a

^a Laboratoire de Biotechnologies Végétales Appliquées à l'Amélioration des Cultures, Faculté des Sciences de Sfax, Université de Sfax, Sfax, Tunisia

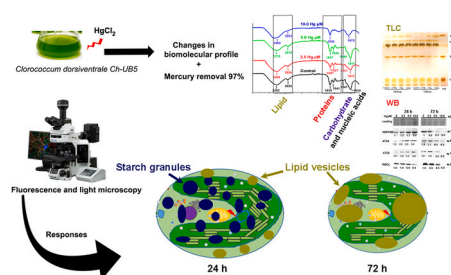
^b Laboratory of Plant Physiology-Department of Biology, Universidad Autónoma Madrid, Darwin 2, ES28049, Madrid, Spain

^c Laboratoire de Génie Enzymatique et Microbiologie, Equipe Biotechnologie des Algues, Ecole Nationale d'Ingénieurs de Sfax, Université de Sfax, Sfax, Tunisia

HIGHLIGHTS

- Mercury removal capacity of *Chlorococcum dorsiventrale* was over 90% after 72 h of exposure.
- The adverse effects of Hg on *C. dorsiventrale* were time and concentration dependent.
- Mercury induced non-specific defenses, such as autophagy, HSP70B, and redox enzymes.
- FTIR spectroscopy highlighted alteration in the biomolecular profile composition (lipids, polysaccharides, and proteins).
- Mercury affected photosynthesis and respiration, altering carbon metabolism and starch and lipid droplets distribution.

GRAPHICAL ABSTRACT



ARTICLE INFO

Handling Editor: Willie Peijnenburg

Keywords:

Chlorococcum dorsiventrale
Microalgae
Mercury
Metabolism
Oxidative stress

ABSTRACT

Mercury (Hg) is a global pollutant that affects numerous marine aquatic ecosystems. We isolated *Chlorococcum dorsiventrale* Ch-UB5 microalga from coastal areas of Tunisia suffering from metal pollution and analyzed its tolerance to Hg. This strain accumulated substantial amounts of Hg and was able to remove up to 95% of added metal after 24 and 72 h in axenic cultures. Mercury led to lesser biomass growth, higher cell aggregation, significant inhibition of photochemical activity, and appearance of oxidative stress and altered redox enzymatic activities, with proliferation of starch granules and neutral lipids vesicles. Such changes matched the biomolecular profile observed using Fourier Transformed Infrared spectroscopy, with remarkable spectral changes corresponding to lipids, proteins and carbohydrates. *C. dorsiventrale* accumulated the chloroplastic heat shock protein HSP70B and the autophagy-related ATG8 protein, probably to counteract the toxic effects of Hg. However, long-term treatments (72 h) usually resulted in poorer physiological and metabolic responses, associated with acute stress. *C. dorsiventrale* has potential use for Hg phytoremediation in marine ecosystems, with

* Corresponding author.

E-mail address: luis.hernandez@uam.es (L.E. Hernández).

the ability to accumulating energetic reserves that could be used for biofuel production, supporting the notion of using of *C. dorsiventrals* for sustainable green chemistry in parallel to metal removal.

1. Introduction

Marine ecosystems are worth assets contributing to the prosperity of many coastal communities that may be at risk due to contamination (Weis, 2015), being one of the most striking environmental disturbances the accumulation of heavy metals in areas with high anthropogenic activity (Zamora-Ledezma et al., 2021), prone to suffer adverse ecological and human health problems due to their persistence and bioaccumulation in the trophic chain of aquatic ecosystems (Zaynab et al., 2022). The Mediterranean basin is particularly at serious risk, very vulnerable to metal contaminants originating in shipping activities, urban, port and riverine effluents inputs, where environmental footprint assessment is of great importance (Merhaby et al., 2019). Several coastal areas in Tunisia, including Sfax, Monastir and the Gulf of Gabes, have been exposed to intense anthropogenic pressure for years, causing serious damages to the coastal ecosystems (Annabi-Trabelsi et al., 2021; Ben Amor et al., 2020; Mosbahi et al., 2019), where there has been an enrichment of Cd, Cu, Ni, Fe, Pb or Cr in sediments nearby harbors and fisheries (Aydi et al., 2022; Rebai et al., 2022). Moreover, there were remarkable high levels of Hg in sediments of various coastal areas in Mahdia (Jebara et al., 2021), Sfax (Cherif et al., 2020) and the Gulf of Tunis (Ben Mna et al., 2021), eventually affecting fishery products (Zrelli et al., 2021; Jebara et al., 2021), which may cause human health complications, including neurological damage and reproductive problems (Ghosh et al., 2022).

Phytoplankton is the foundation of the food web in marine ecosystems, which is comprised among others by microalgae, primary producers that may constitute a key entry point of Hg in the marine trophic chain (Le Faucheur et al., 2014). The susceptibility of those microorganisms can be exploited as bioindicators of pollution, whereas their ability to bioaccumulate trace metals opens the possibility to develop phycoremediation strategies to limit contamination in aquatic ecosystems (Renuka et al., 2015). Phycoremediation is an emerging sustainable decontamination technology that is attracting the interest of researchers (Hamed et al., 2022; Leong and Chang, 2020), but must be optimized through the selection of tolerant microalgae strains (Elleuch et al., 2021a,b; Zada et al., 2022). In the presence of metals, the microalgae biomass growth is compromised with substantial alterations in their metabolism (Leong and Chang, 2020). Apart from these common symptoms, the exposure to Hg leads to inhibition or inactivation of several enzymes due to the strong affinity of this metal for cysteine residues of proteins through the thiol functional group, thereby disturbing vital functions in plant cells and algae (Nesci et al., 2016). Mercury toxicity appears also after a rapid generation of reactive oxygen species (ROS), which are responsible for the obliteration of essential metabolic processes, ultimately leading to the breakdown of the cell (Ajitha et al., 2021; Barón-Sola et al., 2021). Membrane-bound NADPH oxidase (NOX), defined as electrogenic protein that catalyzes the conversion of O_2 to superoxide ions, seems an important source of ROS ($O_2^{\bullet-}$, H_2O_2 and OH^{\bullet}) (Liu et al., 2022). To counteract excessive levels of ROS, microalgae can activate a complex antioxidant defense, which includes several redox enzymes, such as superoxide dismutase (SOD), catalase (CAT), glutathione peroxidase (GPX), ascorbate peroxidase (APX), or glutathione reductase (GR) in the presence of metals like Cd, Cu, Pb or Zn (Kováčik et al., 2017; Choudhary et al., 2007); response that is partially depending on the expression of their genes (Elleuch et al., 2021a,b; León-Vaz et al., 2021). On the other hand, heat shock proteins (HSP) constitute another non-specific defense mechanism, mainly involved in protein folding and protection that contribute to cellular homeostasis (Chankova et al., 2014). Autophagy activation constitutes another protective strategy during heavy metal stress able to recycling

damaged organelles and biomolecules (Barón-Sola et al., 2021; Kajikawa and Fukuzawa, 2020). Autophagy related proteins like ATG8, part of the autophagosome formation complex, can be used as marker of autophagy induction and accumulates in microalgae subjected to several abiotic stress conditions, including metal toxicity (Pérez-Pérez et al., 2017).

Due to cellular damages caused by ROS, turnover and recycling of materials under Hg stress may lead to substantial changes in the biomolecular profile of microalgae that can be detected *in vivo* by Fourier Transform Infrared Spectrometry (FTIR), which is a not invasive technique used to detect changes in the lipids, carbohydrates, and proteins profile in microalgae (Razzak et al., 2022), as observed in *Chlamydomonas reinhardtii* (Barón-Sola et al., 2021) and *Cosmarium* sp. (Shi et al., 2023). Under extreme environments, microalgae can respond by inducing the biosynthesis of neutral lipids (Song et al., 2022), which could be exploited for biofuel production through transesterification reaction (Yang et al., 2015). Therefore, the selection of suitable microalgae for phycoremediation and the accumulation of value-added bio-products is an appealing option for future strategies to clean-up metal polluted aquatic environments.

Limited studies have been carried out to understand the mechanisms of toxicity and tolerance to Hg in microalgae, which could be exploited to optimize phycoremediation strategies (Aravind et al., 2023), particularly by isolating microalgae from marine ecosystems polluted with Hg. Thus, we isolated a novel *Chlorococcum* sp microalga strain from Tunisia coastal regions facing worrisome episodes of Hg contamination. Exposure of this strain to sub-lethal doses of Hg led to remarkable alterations in the biomolecular profile, redox balance and metabolic adjustments that could help to withstand the toxicity of this hazardous metal, probably useful for the optimization of Hg phycoremediation strategies.

2. Material and Methods

2.1. Algal strain isolation and growth conditions

A green algae strain (*Chlorococcum dorsiventrals* Ch-UB5) was isolated from a benthonic sample collected in February 2018 from the Tunisian Coast of Mahdia, where large levels of trace metals were observed. Axenic uniclonal culture was obtained by serial dilutions followed by micromanipulations (Elleuch et al., 2021a,b; Mohamed et al., 2021). Microalgae *Chlorococcum dorsiventrals* cultures were grown in modified F/2 medium and maintained at 22 ± 2 °C under continuous photon flux density of $80 \mu\text{mol photons}\cdot\text{m}^{-2}\cdot\text{s}^{-1}$.

2.2. Strain molecular identification

We extracted the microalgae genomic DNA using PureLink™ purification kit (Teknovas SA, Derio, Spain). DNA quantity and quality were assessed with a NanoDrop 2000 spectrometer (Thermo Fisher Scientific, Waltham, MA, USA). The amplification of 18S rRNA fragment was performed by PCR using the universal Eukarya forward 5'-AACCTGGTTGATCCTGCCAGT-3' and reverse 5'-TGATCCTTCTGCAGGTTACCTAC-3' primers (Ben Amor et al., 2017). The PCR product was analyzed that was purified using MiniElute Gel Extraction Kit (Qiagen, Venlo, The Netherlands) after electrophoresis in 1% agarose gel. The amplicon was sequenced using a taq DyeDeoxy terminator cycle Sequencing kit and a 3700 ABI Prism DNA sequencer (Applied Biosystems, Foster City, CA, USA). Sequences were compared with those available in GenBank using the BLAST tool from NCBI.

2.3. Mercury biosorption test and analysis

Preliminary screening tests were performed in clear glass tubes containing 10 mL of F/2 medium, inoculated with *Chlorococcum dorsiventrals* at an initial cell density of 10^6 cells per mL, and treated with different Hg concentrations using a HgCl_2 30 mM stock solution. Microalgae grew as described above and total cell number (cell/mL) were recorded each 24 h for 3 d (see supplementary Material and Methods information). The half maximal inhibitory concentration (IC_{50}) values were calculated using cell number and the online calculator AAT Bioquest (<https://www.aatbio.com/tools/ic50-calculator>).

Mercury was analyzed in 20 mL cultures grown in for 24 and 72 h Hg. After centrifugation at $10,000\times g$ for 10 min, pellets were air-dried and Hg concentration was quantified using a DMA-80 Mercury Analyzer (Milestone SRL, Sorisole, Italy). In addition, we also analyzed remaining Hg in the supernatant, filtered using a $0.4\ \mu\text{m}$ membrane and stored at 4°C (Elleuch et al., 2021b).

2.4. Zeta potential

Aliquots of *C. dorsiventrals* cultures were diluted in deionised water to a 750 nm OD of 0.1, and 1 mL of the homogenate was added to a Zetasizer Nano (Malvern Panalytical Ltd., Malvern, UK) electrophoretic cell chamber. Zeta potential (ZP) measurements were using 80 mV at 25°C . ZP values were the average of 5 independent runs (Pandey et al., 2019).

2.5. Pigment quantification

Total chlorophyll and carotenoids were quantified by spectrophotometry, using 1 mL methanol extracts using from 60 mg of dried microalgae, after 15 min sonication and overnight incubation at -20°C . The absorption was measured at 666, 653 and 470 nm and the pigment concentration was calculated using the Lichtenthaler equations (Lichtenthaler, 1987).

2.6. Photochemical activity

Photosynthetic activity was examined by maximum oxygen release/consumption rates using a Clark electrode oximeter (Hansatech, King's Lynn, UK) (Clark et al., 1953). two mL of microalgae cells culture were washed twice with Milli-Q water, diluted in HEPES pH 7.4, and dissolved O_2 was exhausted using an argon gas stream in the electrode chamber maintained at constant temperature (22°C). Cells were then supplied with 40 mM NaHCO_3 to trigger photochemical reactions under saturating white light ($300\ \mu\text{mol photons}\cdot\text{m}^{-2}\cdot\text{s}^{-1}$). Oxygen release was measured over an interval of 5 min, while O_2 consumption was measured in the dark. Photosynthetic rates were calculated on the base of total chlorophyll content ($\mu\text{mol O}_2\cdot\text{mg chl}^{-1}\cdot\text{h}^{-1}$) as the algebraic sum of O_2 released in the light plus O_2 consumed in the dark.

2.7. Microscopic analysis and measurements

Microalgae cells were stained with 100 μM H_2DCFDA for oxidative stress detection, 100 μM BODIPY 505/515 for neutral lipids accumulation and 1% lugol for starch granules distribution. Microalgae aliquots were mixed in 1% agarose low melting temperature (LMT) before image analyses and mounted in glass slides. Images were recorded in bright field, FITC filter and red channel for chlorophyll autofluorescence, using an epifluorescence microscope BX63 equipped with a DP74 camera (Olympus, Tokyo, Japan), using CellSens imaging software (Olympus). Simultaneously, 200 μL of cells cultures were placed in a 96-well black microtiter plate to measure Chl-a fluorescence (630–750/20 nm excitation/emission wavelength filters), BODIPY 505/515 and H_2DCFDA fluorescence (485–528/20 nm excitation/emission filters) using a Synergy HT Reader (BioTek, Winooski, VT, USA).

2.8. Lipid peroxidation

Lipid peroxidation was determined spectrophotometrically by measuring the concentration of thiobarbituric acid reactive substances (TBARS) (Buege and Aust, 1978). 10 mL of the microalgae cultures were centrifuged at $12000\times g$ for 15 min at 4°C . Samples were homogenized in 1 mL trichloroacetic acid (TCA) solution (0.1%), the homogenate was centrifuged for 30 min and 0.5 mL of supernatant was mixed with 0.5 mL of 0.5% TBA–HCl reagent. The mixture was boiled at 90°C for 30 min in water bath, immediately cooled on ice, and centrifuged at $10,000\times g$ for 10 min. Further, the absorbance of the resulting chromophore was measured at 532 nm using UV/VIS Pharo 300 spectrophotometer (Merck, Readington, NJ, USA). The TBARS concentration was calculated directly from the extinction coefficient, subtracting unspecific absorbance at 600 nm (Carrasco-Gil et al., 2023).

2.9. Total phenolic content

Phenolic compounds were extracted from fresh microalgae samples in 50% ethanol for 15 min at 60°C . Total phenolic concentration was determined using Folin-Ciocalteu reagent (Meyers et al., 2003), by mixing 100 μL of the ethanolic extract with 750 μL 6% NaHCO_3 . Subsequently, 750 μL diluted Folin–Ciocalteu reagent (1:10) were added and allowed to stand at room temperature for 90 min. The absorbance was measured at 750 nm, and concentration was calculated against a gallic acid standard curve (Vinson et al., 1998).

2.10. Immunodetection of proteins of interest

Proteins were extracted from microalgae pellets stored at -80°C following a series of quick freezing and thawing cycles in liquid nitrogen in a protein extraction buffer composed of 30 mM MOPS, 10 mM DTT, 5 mM EDTA, PMSF 0.06% (w/v) and protease inhibitor cocktail (Ref. P2714, Sigma- Aldrich, St. Louis, MO, USA) (Ortega-Villasante et al., 2021). The homogenate was centrifuged ($10,000\times g$ at 4°C for 15 min), the supernatant distributed in several aliquots and protein was quantified using the Bradford reagent (BioRad, Hercules, CA, USA) (Bradford, 1976). Proteins of interest were immunodetected by Western-blot analysis using 10 μg of proteins, separated by electrophoresis in 10% sodium dodecyl sulfate polyacrylamide gel (SDS-PAGE) (Elleuch et al., 2016a,b). Proteins were electroblotted onto nitrocellulose membrane (Thermo Scientific, Germany) using wet tank blotting system Mini Trans-Blot® Cell (Bio-Rad) and exposed separately to the following commercially available primary antibodies (Agrisera, Vännäs, Sweden): GR (AS06181); CAT (AS152991); APX (AS06180); NADPH (AS204427); ATG8 (AS142769); ATG4 (AS152831); RbcL (AS03037) and HSP70B (AS06175), using recommended dilutions of each antibody and the procedures described by Barón-Sola et al. (2021). Specific bands were detected after incubation for 2 h with the secondary HRP Goat Anti-Rabbit IgG antibody (Agrisera) diluted to 1:10000 in washing buffer, and the immune complex was revealed using the Western blotting detection kit (LumiSensor, Ref. L00221V300, GenScript) with a ChemiDOC XRS+ (BioRad) system. Densitometric analysis and image acquisition were performed to determine the intensity of the immunoreactive bands using the Image Lab software (Version 6.1, Bio Rad).

2.11. Redox enzymatic activities

Determination of redox enzymatic activity was performed after non-denaturing protein gel electrophoresis (ND-PAGE) of protein extracts, 20 μg protein per sample were loaded and electrophoretic separation was performed in non-denaturing condition at 4°C for 4 h with a constant current of 60 mA (Elleuch et al., 2016a,b). The polyacrylamide concentrations used were 8% for CAT, and 10% for GR and NADPH oxidase. To visualize catalase activity, the electrophoresed gels were treated with 0.01% hydrogen peroxide (H_2O_2) and then incubated in a

mixture of 2% ferric chloride (FeCl_3) and 2% potassium ferric cyanide (K_3FeCN_6) for 30 min. GR activity was assayed by incubating gels in GR staining solution containing 250 mM Tris-HCl buffer (pH 7.5) supplemented with 0.5 mM NADPH, 3.5 mM oxidized glutathione (GSSG), 0.2 mg mL^{-1} 2,6 dichlorophenolindophenol (DCPIP) and 0.2 mg mL^{-1} 3-(4,5-dimethyl-2-thiazolyl)-2,5-diphenyl-2H-tetrazolium bromide (MTT) for 1 h at room temperature (Sobrinho-Plata et al., 2014). For NADPH oxidase activity, native gels were stained using the NBT reduction method, in gels incubated in the dark for 30 min in a reaction staining mixture containing 250 mM Tris-HCl buffer (pH 7.5), supplemented with 0.5 mg mL^{-1} NBT, 0.2 mM MgCl_2 , 4 mM CaCl_2 and 0.2 mM NADPH.

2.12. Biomolecular profile by FTIR analysis

Dried microalga pellets (10 mg) were ground with KBr powder (1 g) and scanned using a FTIR Cary 630 Spectrometer (Agilent Technologies, Santa Clara, CA, USA) to identify functional groups based on their absorption bands ranging between 400 and 4000 cm^{-1} wavenumber, with 32 scans having 4 cm^{-1} spectral resolution.

2.13. Thin layer chromatography for lipid analysis

Lipids were extracted using 80 mg fresh cells biomass in 1 mL lipid extraction solvent (methanol/chloroform/formic acid; 20:20:0.2; v/v/v), which were disrupted using an ice-cooled Potter-Elvehjem glass homogenizer. The resulting extract was washed two times with 1 mL washing solvent mixture (chloroform/methanol/0.6 M formic acid; 0.6:9.6:9.4; v/v) and centrifuged at 13,500 \times g, 15 min at 4 °C to separate the upper organic phase. The organic phase was transferred to a 4 mL glass vial, and the solvent was evaporated under a stream of nitrogen (g). The dried residue was then dissolved in chloroform/methanol (1:1; v/v) to a final chlorophyll concentration of 10 $\mu\text{g}/\mu\text{L}$. Equal amount of chlorophyll (40 μg) were spotted on a TLC silica gel plate (Sigma-Aldrich), and lipids were eluted using a two solvent procedure, firstly (2/3 elution) with acetone/toluene/ H_2O (91:30:3; v/v/v), followed by a second elution step with hexane/diethyleter/glacial acetic acid (70:30:1; v/v/v). Lipid spots were visualized using iodine vapor and were identified in comparison to the migration of available standards.

2.14. Statistical analysis

One-way Anova followed by post-hoc Tukey's test were used to establish the statistical significance, using the IBM SPSS Statistics software (version 22). Shapiro-Wilk and Kolmogorov-Smirnov tests were done to confirm normal distribution of variables. The p -values <0.05, 0.01, and 0.001 were marked by *, ** and ***, respectively.

3. Results and discussion

3.1. Microalgae strain characterization

Based on the morphological taxonomic criteria of microalgae (https://www.algaebase.org/search/genus/detail/?genus_id=37477), the isolated microalgae Ch-UB5 is a member of the genus *Chlorococcum*, unicellular with a characteristic single cup-shaped parietal chloroplast with a single pyrenoid (Fig. S1A). This morphological identification was completed by its molecular identification, based on eukaryotic 18S rDNA genomic region amplification and sequencing. The 18S rDNA sequence of Ch-UB5 strain was BLAST compared with DNA sequences available in the GenBank database (<https://www.ncbi.nlm.nih.gov/>), and affiliated to *Chlorococcum* genus and *dorsiventrals* species, with a 100% identity to AB058302.1 accession (Fig. S2). The strain showed a good self-settling rate of 85% after a relatively short time of 3 h at pH 7.4. The self-sedimentation rate was found to be higher and faster than those previously reported for *Chlorella vulgaris* (55.45% after 4 h)

(Elleuch et al., 2021a,b) and *Ankistrodesmus falcatus* (74.65% after 24 h) (Zheng et al., 2019).

3.2. Inhibitory concentration, morphological changes and Hg biosorption capacity

Preliminary screening, through half maximal inhibitory concentration (IC_{50}) determination, showed the tolerance of *C. dorsiventrals* to a range of heavy metals, particularly Hg (data not shown). The obtained IC_{50} of *C. dorsiventrals* against Hg was 1.315 mg/L equivalent to 5 μM HgCl_2 . $\frac{1}{2}\text{IC}_{50}$, IC_{50} and $2\times\text{IC}_{50}$ were used for further experiments to evaluate physiological changes in *C. dorsiventrals* cells after short- (24 h) and long-term (72 h) Hg exposures, enabling us to compare mild stress versus acute stress situations.

The removal efficiency of this strain reached 87% and 97% after 24 and 72 h Hg treatments, respectively, following a dose pattern (Table 1). Previous studies reported the effectiveness of *Chlorococcum* genus in biosorption of Cu, As, Cd and Pb (Liyanage et al., 2020; Qiu et al., 2022; Upadhyay et al., 2022), but information about Hg removal using this microalga is scarce. This bioaccumulation depends on the interaction of metals with macromolecular compounds located in cell walls and intracellular compartments (Yang et al., 2015). In this sense, microscopic observation showed that under Hg stress there were clear morphological damages visible after 24 and 72 h of treatment: cells appeared with irregular shapes, shrank, lipid vesicles and the shape of the blebbing cells, the size and their pyrenoids were severely altered, in comparison with control cells (Fig. S1). There was also clear cell aggregation/flocculation observed after 24–72 h of exposure to Hg, as was shown by the Zeta Potential (ZP) values, with high electronegativity values in control cells (−33 mV) that reflected the dispersing stability of cells. However, measurements of the ZP of *C. dorsiventrals* showed a significant increase of cell surface charge values (less electronegative) as a function of exposure times and Hg concentrations (2.5–10 μM), reflecting subsequent flocculation of cells in Hg treated cultures (Supplementary Fig. S3).

3.3. Biomass growth and pigment concentration

Several physiological fingerprints were examined, such as biomass, photosynthetic pigments, oxygen release and respiration, to evaluate the toxic effect of Hg on *C. dorsiventrals*. The strain growth biomass was substantially inhibited by different HgCl_2 concentrations (2.5, 5 and 10 μM), with a drastic diminution of 67% after 24 h of treatment with 10 μM HgCl_2 , and was almost completely suppressed (90%) after 72 h (Fig. S4). In concordance, several studies reported that Hg is highly toxic element, inhibiting cells growth even in trace concentrations (Hazlina et al., 2019; Wang et al., 2022).

The level of photosynthetic pigments is frequently used as biomarker of environmental stressors in microalgae. Chlorophyll (a, b and total) concentrations dropped acutely in a dose-dependent manner after 24 and 72 h of exposure to Hg (Fig. 1A, B, 1C). Similarly, *Nannochloropsis oculata* and *Chlorella vulgaris* showed chlorosis symptoms when treated with Hg (Hazlina et al., 2019; Zamani-Ahmadmahmoodi et al., 2020). Consistently, previous studies also showed that total carotenoids

Table 1
Removal percentage and quantification of adsorbed and intracellular Hg content in treated *C. dorsiventrals* with different Hg concentrations (2.5, 5 and 10 μM) after 24 and 72 h of incubation.

	HgCl_2 (μM)	Removal (%)	Biosorbed ($\text{Hg } \mu\text{mol} \cdot \text{g}^{-1} \text{ DW}$)
24 h	2.5	87 \pm 0.3	2.602 \pm 0.070
	5	87 \pm 1.9	4.624 \pm 0.130
	10	63 \pm 4.1	9.103 \pm 0.018
72 h	2.5	95 \pm 0.3	2.816 \pm 0.095
	5	97 \pm 0.1	4.697 \pm 0.408
	10	97 \pm 0.2	7.307 \pm 0.299

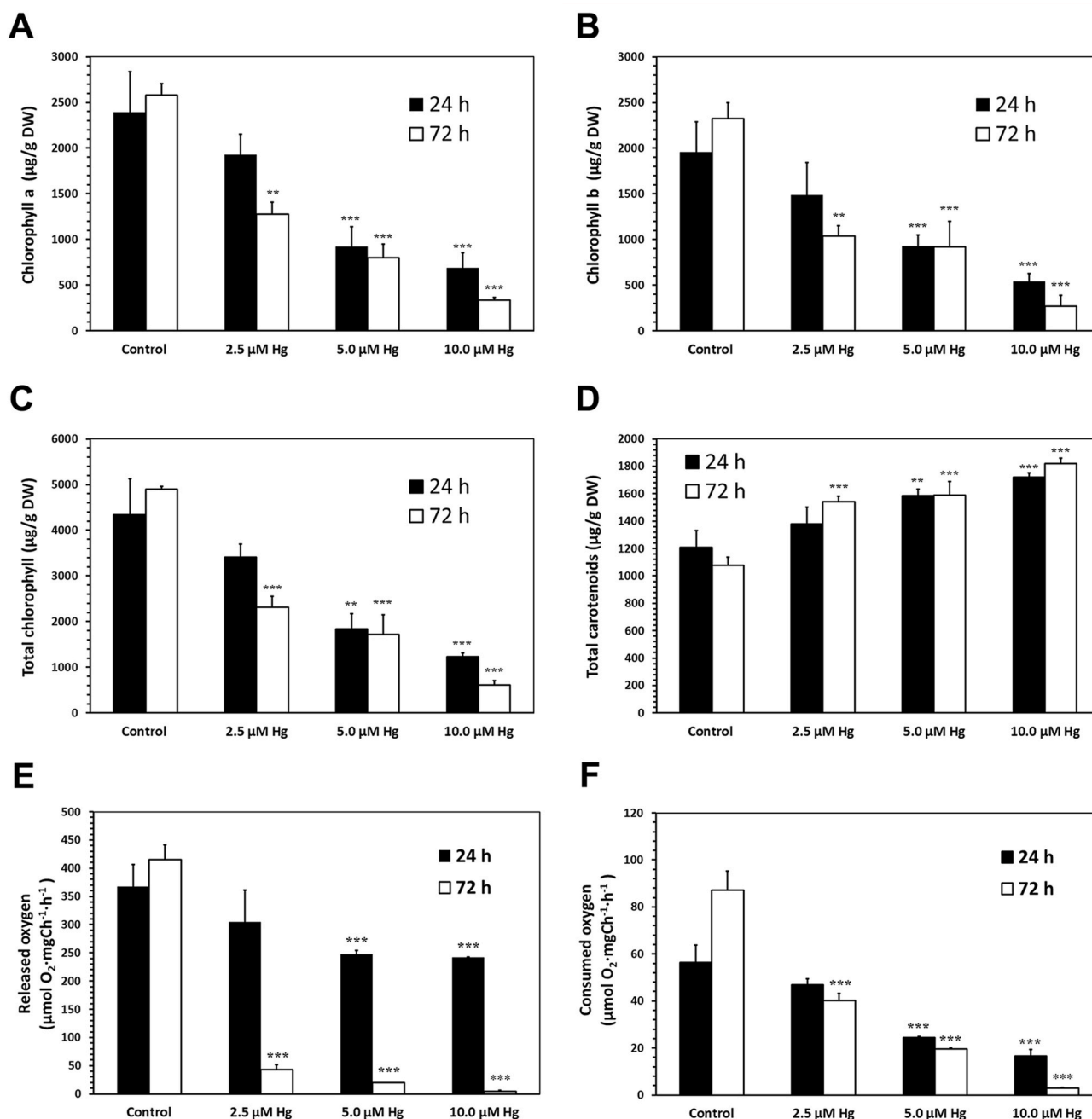


Fig. 1. Effect of Hg on photosynthetic activity of *C. dorsiventrals* after 24 and 72 h treatment with 0 (control), 2.5, 5 and 10 µM Hg. **A, B and C**) Chlorophyll-a, chlorophyll-b and total chlorophyll content (mg g^{-1} DW). **D**) Total carotenoids content (mg g^{-1} DW). **E**) Maximum oxygen release rate ($\mu\text{mol O}_2 \text{ mg Chl}^{-1} \text{ h}^{-1}$). **F**) Maximum oxygen consumption rate ($\mu\text{mol O}_2 \text{ mg Chl}^{-1} \text{ h}^{-1}$). Bars represent the standard error of three independent biological replicates, and asterisks indicate statistical differences (* $p < 0.05$; ** $p < 0.01$; *** $p < 0.001$).

concentration in *Nannochloropsis oculata* increased in response to Hg, Pb, and Cd stress (Zamani-Ahmadm Mahmoodi et al., 2020). It was also reported that the decrease in chlorophyll content might be due to the substitution of the central Mg^{2+} by heavy metal ions (Grajek et al., 2020; Zamani-Ahmadm Mahmoodi et al., 2020). In addition, carotenoid concentration increased significantly in Hg-treated cells (Fig. 1D). Carotenoids have antioxidant activity to counteract the free radicals occurring in chloroplasts and may help to limit the damages triggered by Hg in this organelle (Danouche et al., 2022; Hamed et al., 2019).

In vivo analysis of chlorophyll *a* fluorescence was assayed to examine the toxicity of Hg ions. Red self-fluorescence of chlorophyll decreased gradually under Hg stress, particularly drastic in 10 µM Hg-treated cells after 72 h (Fig. 2A). The results showed high correlation between HgCl_2

doses and chlorophyll *a* fluorescence intensity, in accordance with the values of pigment concentration (Fig. 2B). Similar results were reported for microalgae cells subjected to various stress conditions (Maldonado et al., 2010; Seoane et al., 2017).

3.4. Photochemical activity and respiration

The changes in photosynthetic pigments could be related with alteration in photochemical processes in the presence of Hg, resulting in the disturbance of cellular homeostasis (Grajek et al., 2020; Nowicka, 2022), where there could be an inhibition of the electron transfer chain between PSII and PSI (Yan et al., 2021; Yong et al., 2021; Seoane et al., 2017). The O_2 release rate decreased significantly in microalga treated

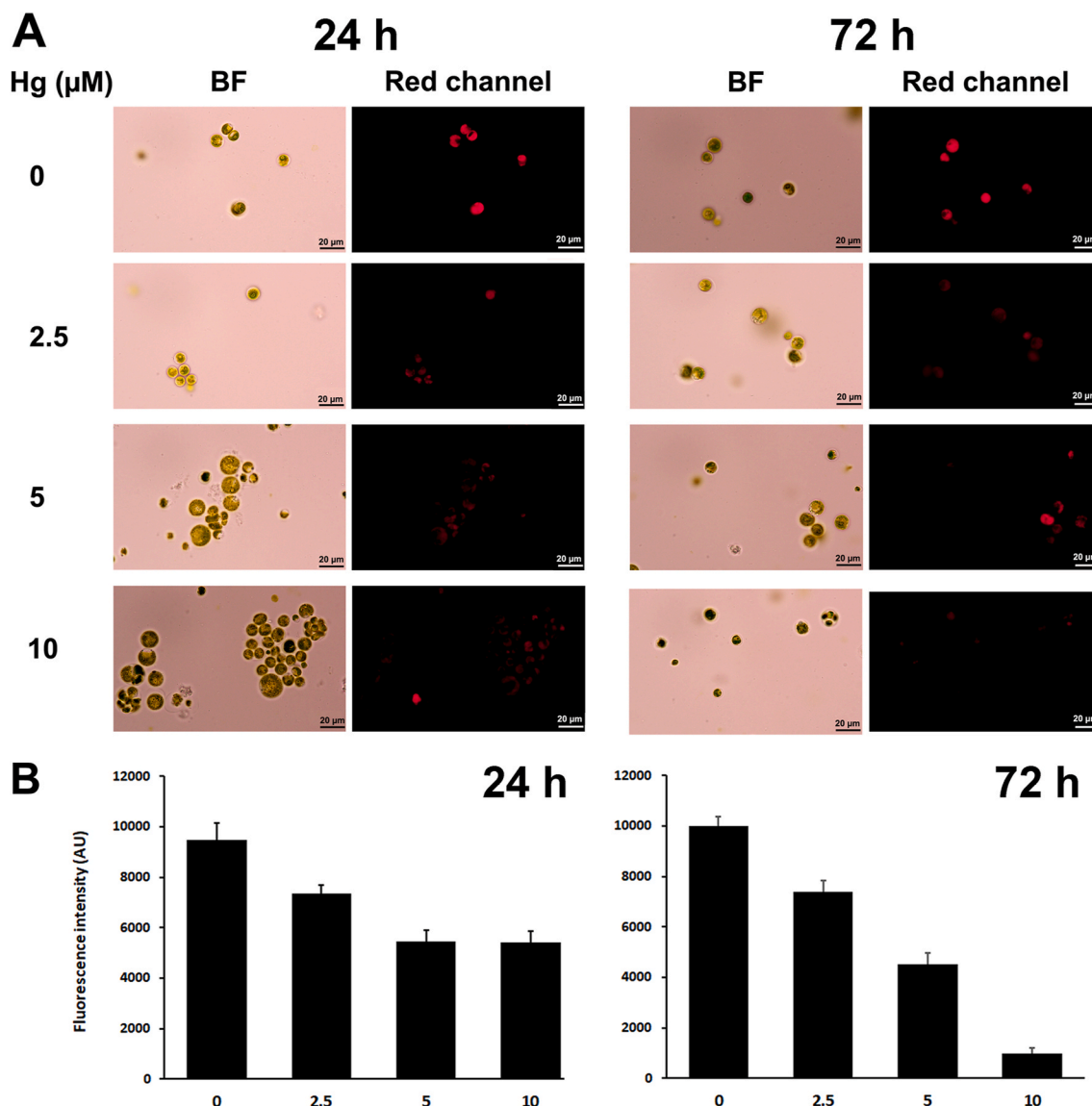


Fig. 2. A) Chlorophyll autofluorescence (red channel) and bright field (BF) images of *C. dorsiventrals* cells before and after exposure to different doses of Hg (0, 2.5, 5 and 10 μM) and exposure time (24 and 72 h). Scale bar = 20 μm. B) Chlorophyll autofluorescence intensity (arbitrary units, AU) of *C. dorsiventrals*. Error bars represent S.D. of three independent experiments. (For interpretation of the references to color in this figure legend, the reader is referred to the Web version of this article.)

with 5 and 10 μM Hg (up to 30% of the controls) after only 24 h, whereas it plummeted by more than 90% in cells exposed even at the lowest dose (2.5 μM) after 72 h (Fig. 1E). Therefore, Hg stress affected the oxygenic reactions at PSII. Similarly, *Chlamydomonas reinhardtii* showed that photosynthetic machinery is highly sensitive to Hg stress, where O_2 release rate dropped more than in the presence of Cd (Barón-Sola et al., 2021). It seems that Hg is more toxic than Cd, due to the differential susceptibility of PSII and PSI to Cd-stress (Bartolomé et al., 2016). The oxygen evolution complex (OEC) is an important parameter reflecting the PSII photosynthetic efficiency (Cardol et al., 2011; Wang et al., 2021a, b), and could lead to detrimental energy conversion during the photochemical reactions in *Chlorella vulgaris* incubated with the stressor cetyltrimethyl ammonium chloride, which resulted from limited electron flow between OEC and PSII (Liu et al., 2020).

Consumption of O_2 under dark conditions (respiration rate) was also significantly inhibited in the presence of $HgCl_2$ (Fig. 1F). Therefore, the mitochondrial electron respiratory chain was also sensitive to Hg exposure. Some authors suggest that this could be due to the dysfunction of the mitochondrial respiratory chain due to Hg-thiol interactions

(Nesci et al., 2016).

3.5. Oxidative stress

ROS species accumulate in the chloroplast and mitochondria in photosynthetic organisms specially under stress, which results in cellular redox imbalance (Coulombier et al., 2021). Oxidative stress was analyzed in *C. dorsiventrals* treated with Hg using H_2DCFDA , which bright green fluorescence intensity increased in a Hg concentration-dependent manner after 24 h of incubation (Fig. 3A and B). Similarly, Ajitha et al. (2021) reported that Hg stress induced the formation of ROS in *Chlorella vulgaris*, and hence oxidative damages appeared. However, H_2DCFDA fluorescence intensity decreased remarkably after 72 h of exposure to Hg, particularly in *C. dorsiventrals* treated with 10 μM. This finding could probably be due to loss of metabolic activity in Hg-poisoned cells, ultimately suffering cell death and/or the leak of the fluorochrome probe (Seoane et al., 2017). Similar to our results, long-term exposure to heavy metals inhibited esterase activity in the green alga *Pseudokirchneriella subcapitata* required for

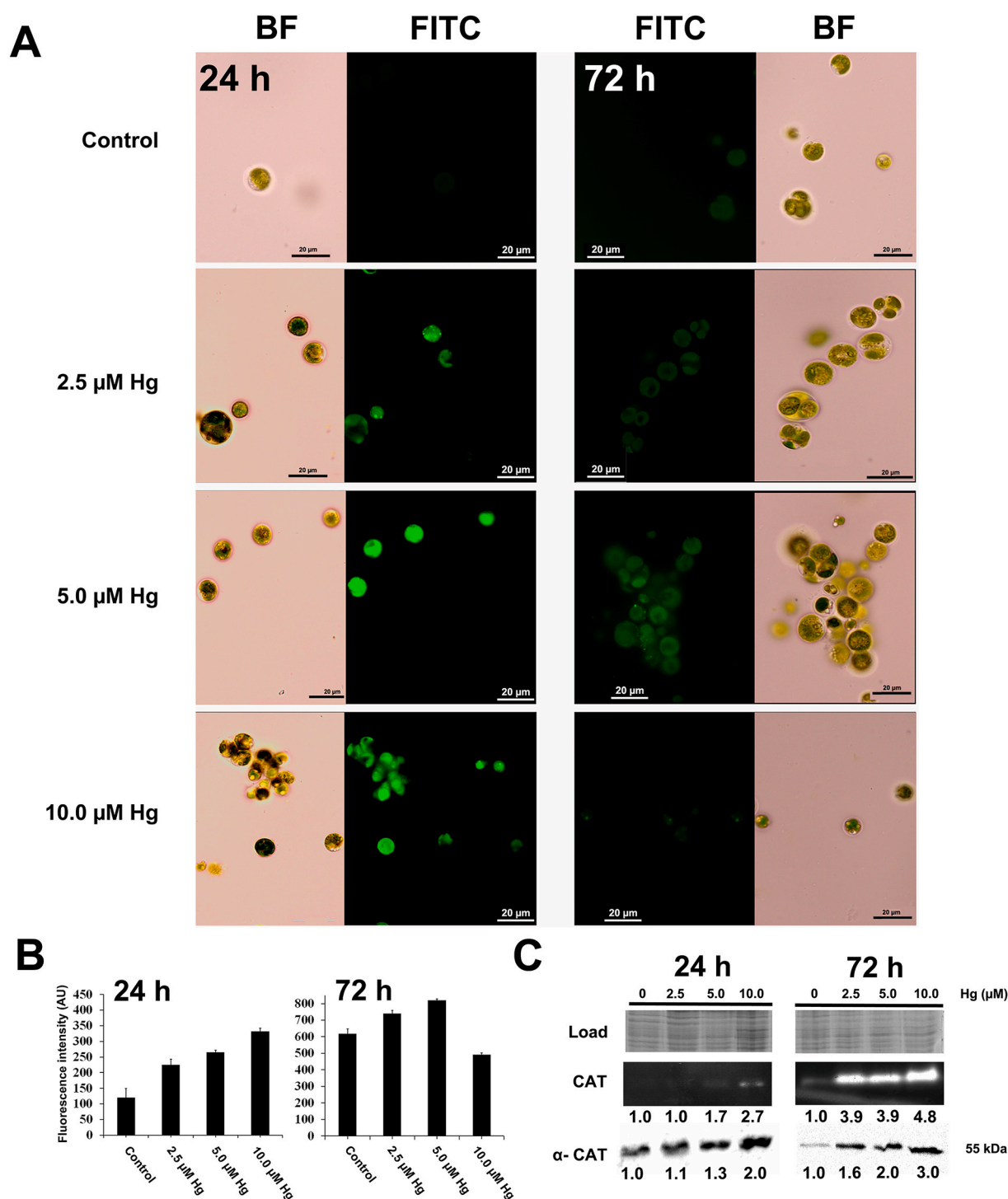


Fig. 3. Oxidative stress evaluated by H_2DCFDA assay and induction of CAT in Hg treated (0, 2.5, 5 and 10 μM) *C. dorsiventrals* for 24 and 72 h. **A)** Fluorescence microscopic images of intracellular ROS content. Scale bar: 20 μm . **B)** Microplate ROS fluorescence intensity, all data are presented as mean value \pm SD of triplicates. **C)** Immunodetection (55 KDa) (α -CAT) and *in gel* activity of CAT from *C. dorsiventrals*. Values of each band represent the fold-changes compared to the control.

metabolization of H_2DCFDA prior reaction with organic peroxides, impeding the subsequent emission of fluoresceine fluorescence (Machado et al., 2015). In addition, lipid peroxidation showed similar pattern with significant rise in TBARS concentration at the highest Hg dose applied after 24 h (Fig. S5), indicating large production of ROS (Danouche et al., 2022; Qiu et al., 2022). Again, after 72 h, TBARS concentration dropped drastically in cells treated with the highest $HgCl_2$ concentration (10 μM), probably due to lost cell integrity due to Hg poisoning.

Pro-oxidant NADPH oxidase (NOX) activity increased significantly after 24 h exposure to Hg but was suppressed after 72 h of treatment under acute stress (Fig. S6). In parallel, the increase in ROS species in Hg treated cells, is also confirmed by the over-accumulation of NOX after short term exposure, which was down-regulated also after 72 h of Hg exposure (Fig. S7A). Similar pattern of NOX and lipid peroxidation occurred in plants and algae in response to different pollutants (Hamed et al., 2022; Zhang et al., 2009), representing a general mechanism that may trigger antioxidant defenses required for cell homeostasis (Huang

et al., 2023; Ortega-Villasante et al., 2018, 2021;).

To cope with the oxidative imbalance caused by toxic metals, several antioxidant defenses were induced, including enzymatic like CAT, APX, and GR (Tripathi and Poluri, 2021; Xiao et al., 2023). CAT and APX possess different affinity for reducing H_2O_2 to maintaining cellular redox homeostasis that varies between species (Anjum et al., 2016). In *C. dorsiventrals*, we mostly found activation of CAT activity under Hg stress, which evidently increased even in cells exposed to 10 μM Hg for 72 h (Fig. 3C), but minor changes occurred in APX activity (data not shown). The amount of CAT, detected by immunodetection, also showed that treatment with Hg clearly induced the expression of CAT (Fig. 3C), matching the role of CAT to alleviating ROS production under metal stress in microalgae (Tripathi et al., 2021). When it comes to the amount of GR and APX, it increased in a Hg dose-manner in both cases after 24 h but dropped at the highest doses of Hg after 72 h (Fig. S7A), which could be due to the degradation of proteins occurring under these conditions (Gill and Tuteja, 2010). Similarly, Hg induced the accumulation of antioxidant enzymes and metabolites in *Chlorella vulgaris* and *Chlamydomonas reinhardtii* (Elbaz et al., 2010). On the other hand, the drop of GR levels caused in poisoned microalgae suggests changes in the cellular levels of reduced glutathione (GSH) versus oxidized glutathione (GSSG) pools, which is critical to maintain the cellular redox balance under metal stress (Gill and Tuteja, 2010).

Regarding several analyzed antioxidant metabolites, we found remarkable accumulation of phenolic compounds (total phenolic concentration) in *C. dorsiventrals* after 24 h treatment with 10 μM Hg (Fig. S7B), concentration that gradually dropped to 50% after 72 h under acute stress. Similar results appeared in *Dunaliella* sp., *Chlorella sorokiniana* and *Scenedesmus acuminatus*, where Zn biosorption induced ROS accumulation and polyphenol biosynthesis (Elleuch et al., 2021a,b; Hamed et al., 2017). Phenolic compounds are known as an effective antioxidant in response to environmental stresses (Rezayian et al., 2019), probably directly inhibiting peroxidation reactions and intervening in H_2O_2 -scavenging reactions catalyzed by redox enzymes, which may attenuate the oxidative damage caused by Hg along with other antioxidant metabolites like carotenoids (Xiao et al., 2023).

3.6. Biomolecular profile

Fourier transformed infrared (FTIR) spectroscopy is a powerful tool to characterize *in vivo* the whole biomolecular profile in microalgae and was used to explore the biomolecular changes of *C. dorsiventrals* associated with Hg stress. The mid-IR spectrum showed the presence of different functional groups with vibrational/stretching wavenumbers: OH (3282 cm^{-1}), C-H (2925 cm^{-1} , 2957 cm^{-1}), C=O (1625 cm^{-1}), C=C (1636 cm^{-1}), P=O (1340 cm^{-1} , 1240 cm^{-1}) and COO- (1019 cm^{-1}), characteristic of lipids, proteins, carbohydrates, nucleic acids and carbohydrates in control and Hg treated cells (Table S1). There were notable peak shifts in the presence of Hg (2.5, 5 or 10 μM), in comparison with the non-treated control, reflecting several alterations in the composition of lipids, carbohydrates and proteins (Fig. 4A and B), characteristic of heavy metals stress in microalgae (Shi et al., 2023). Changes in infrared bands in lipid regions ($2800\text{--}3000\text{ cm}^{-1}$) and the stretching of ester and fatty acid (C=O) spectra (1740 cm^{-1}) after 24–72 h of treatment with Hg could be ascribed to the alteration and modification of lipid composition. Similar alterations in FTIR corresponding to aliphatic chains of fatty acids were also detected in *C. reinhardtii* under Cd and Hg stress (Barón-Sola et al., 2021). Peaks in the spectral region at 1625 and 1520 cm^{-1} , which generally correspond to the carboxylic function (C=O) and (C–N) stretching of proteins (Amide I, amide II) also shifted. This is probably due to the alteration of protein folding and content due to the strong binding capacity of Hg to the thiol groups of cysteines, affecting proper protein folding (Sharma et al., 2008). There were also several peak shifts in the spectral region from 1500 to 900 cm^{-1} , with a $1240\text{--}1247\text{ cm}^{-1}$ peak corresponding to asymmetrical stretching of P=O, present in nucleic acids. Subsequently,

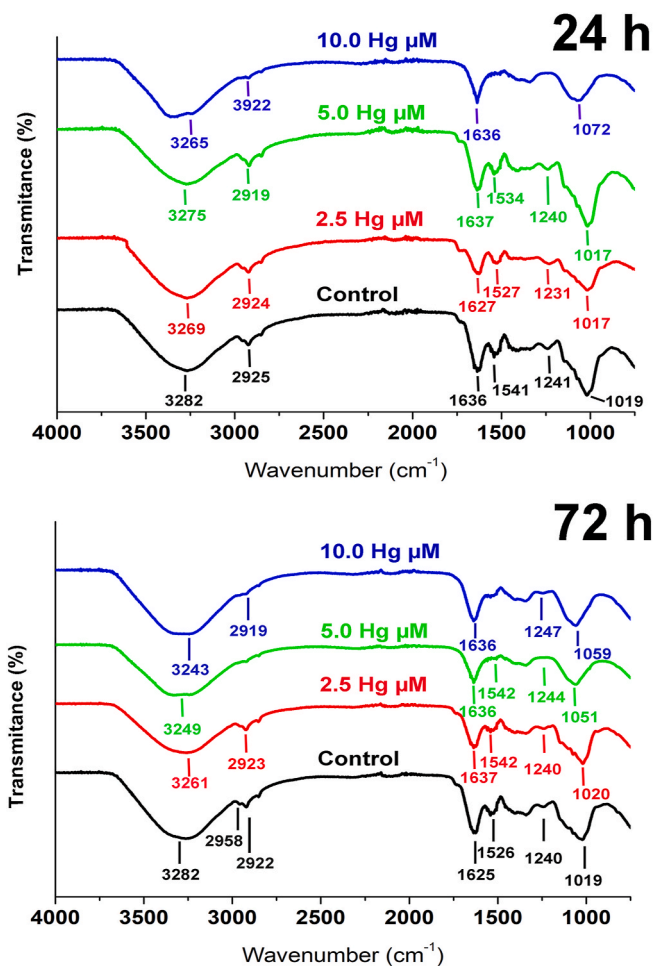


Fig. 4. FTIR analysis of Hg *C. dorsiventrals* cells spiked with Hg (0, 2.5, 5 and 10 μM) for 24 and 72 h of incubation. Numbers indicate the band assignments of the most representative peaks.

the peak at 1019 cm^{-1} observed in control cells shifted towards higher wavenumber in Hg treated cells, which possibly corresponds to C–O–C vibration characteristic of polysaccharides. Significant peak shifts were also observed in carbohydrate and phosphate regions in *Chlamydomonas reinhardtii* under Cd and Hg stress (Barón-Sola et al., 2021). Therefore, FTIR data suggest substantial alterations in carbon metabolism (Charles et al., 2019; Li et al., 2013), known to be adjusted by microalgae under abiotic stress (Paliwal et al., 2017). In this respect, previous studies revealed metabolic disorders such as the dispersion of starch granules and lipid accumulation in *C. reinhardtii* (Barón-Sola et al., 2021) and in *Chlorella vulgaris* (Peng et al., 2017) treated with Hg.

3.7. Stress-related proteins

FTIR data support the idea that changes in the native conformation of proteins occur in microalgae treated with Hg. Heat shock proteins (HSPs) are known as molecular chaperones necessary for proper protein folding, degradation, and membrane translocation (Hartl, 1996; Zhang and Glaser, 2002). In the present study, the stromal heat shock protein (HSP70B) accumulation was estimated by immunoblotting (Fig. 5). The amount of HSP70B was proportional to $HgCl_2$ doses only after 24 h exposure (Fig. 5). In concordance, *Chlamydomonas* cells treated 24 h with Hg or Cd induced HSP70B expression marking the chloroplastic damages degree (Barón-Sola et al., 2021). HSP70B seems a crucial element in the formation of VESICLE-INDUCING PROTEIN PLASTID 1 necessary for maintenance of thylakoid membrane integrity in

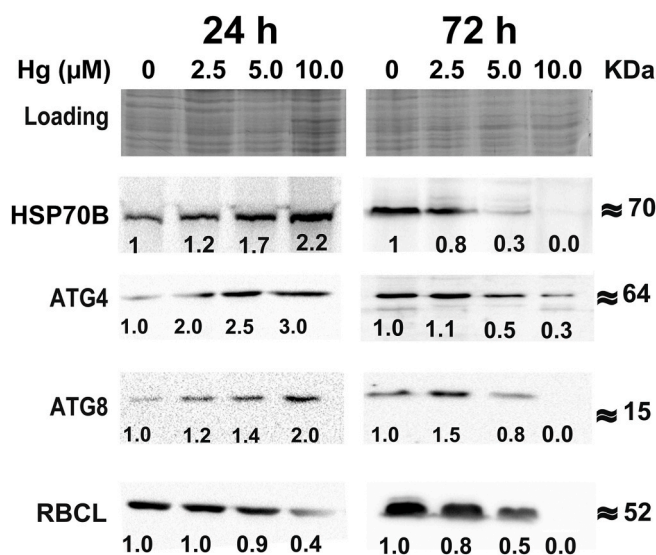


Fig. 5. Western-blot analysis of chloroplast stress damage marker (α -HSP70B), autophagy markers (α -ATG8 and α -ATG4) and rubisco (RbclL) after 24 and 72 h treatments with 0, 2.5, 5 and 10 μ M Hg. SDS-PAGE of denatured proteins shows equivalent sample loading. Specific band signals were quantified relative to the control, and the numbers represent the relative fold-change.

Chlamydomonas under abiotic stress (Liu et al., 2007). However, HSP70B failed to accumulate or even decreased sharply after 72 h. Similar pattern was found for other proteins as discussed below, which could be related with the very strong Hg toxicity that causes degradation of chloroplast components (Chankova et al., 2014).

Along with activation of antioxidant enzymes and chaperone molecular proteins, cells also respond by promoting the degradative pathway: autophagy. In the present study, ATG8 and ATG4 autophagy markers were monitored in *C. dorsiventrals* cells after 24 and 72 h to Hg exposure (Fig. 5). 24 h of Hg exposure led to overexpression of ATG8, marker of autophagosome formation. In a similar way, ATG4 protein content also increased, proving that both proteins act in correlation. The ATG4 paradox protein is known to play a key role in autophagosome biogenesis mainly in ATG8 lipidation and recycling (Pérez-Pérez et al., 2021; Sanchez-Wandelmer et al., 2015). In addition, ROS accumulation and induction of oxidative damage appearing under various biotic and abiotic stresses led to autophagy induction for cell component recycling (Barón-Sola et al., 2021; Kajikawa and Fukuzawa, 2020; Zharova et al., 2022). Regarding cells after 72 h exposure to Hg, both ATG8 and ATG4 levels decreased, which might be concomitant with already described general alterations in different proteins under acute cellular damage and the large changes observed in protein spectral region of 1625 and 1520 cm^{-1} characteristic of Amide I and II detected by FTIR (Fig. 4).

On other hand, the amount of rubisco (ribulose- 1,5-bisphosphate carboxylase-oxygenase) large subunit (RbclL) decreased in a Hg dose-manner after 24 h of treatment, effect that was clearer in *C. dorsiventrals* subjected to strong Hg stress after 72 h (Fig. 5). Therefore, the inhibition of photosynthetic activity found under Hg stress (see Fig. 1E) could be at least partially explained by the loss of rubisco, critical enzyme in the photosynthetic carbon fixation. Consistently with our findings, exposure to Cu^{2+} and CAPTAN (an organochlorine fungicide that is a risk to the environment) led to down-regulation of rubisco in parallel to inhibition of photosynthetic activity *Chlorella vulgaris* and *Nostoc muscorum*, respectively (Andrade et al., 2021; Hamed et al., 2022).

3.8. Starch localization

Due to the changes in the carbohydrate spectra detected by FTIR, we

analyzed the distribution of starch granules in *C. dorsiventrals* and within 24 h of treatment, cells showed proliferation of starch granules (dark blue color; Fig. 6). Starch grains accumulated in a dose dependent manner, especially in cells incubated with 10 μ M Hg where starch occupies almost the whole cell volume. Interestingly, the pyrenoid structure formed by a concentric sheath of starch granules seemed disrupted at this high Hg dose, which appropriate organization is important for adequate function CO_2 concentrating mechanism in microalgae, and hence necessary for CO_2 fixation by rubisco (Penen et al., 2020). Changes in starch metabolism appeared upon exposure to various pollutants in microalgae (Morlon et al., 2005; Shao et al., 2022), and similar disruption of stromal starch granules were observed in *Chlamydomonas reinhardtii* in response to Hg or Cd (Barón-Sola et al., 2021). In addition, long-term exposure (72 h) to Hg led to disappearance or degradation of starch granules in comparison with short-term (24 h) treated cells. This was corroborated by the quantification of total carbohydrates that showed similar pattern: significant increase in cells treated with Hg after 24 h of exposure, but a remarkable depletion after 72 h treatments (Fig. S8). Apparently, our results with Hg stress seem to mimic the symptoms occurring in *Chlorella vulgaris* under nitrogen starvation, where carbohydrate content increased in the short-term stress but decreased after three days of acute stress conditions (Nordin et al., 2020). The toxic effect of Hg on starch metabolism and rubisco stability may be part of an overall alteration of photosynthesis, also observed by the impairment of the photochemical activity, as toxic substances are known to alter the functioning of photosynthetic apparatus and its associated metabolism, resulting in the sensitivity of photosynthetic organisms (Kumar et al., 2014). In particular, Hg is known to cause severe inhibition of the photosynthetic electron transport chain by interfering with different sites such as the water-splitting system and PSI and PSII (Samson and Popovic, 1990), and can be the reason behind the inhibition of the photochemical reactions observed in our experiment (Fig. 1E and F). On the other hand, stressful situations impose changes in the microalgae carbon metabolism where starch can be consumed in favor of biosynthesizing neutral lipids (Kato et al., 2017; Li et al., 2015).

3.9. Lipid metabolism alterations

Neutral lipids accumulation was visualized in single *C. dorsiventrals* cells using the lipophilic BODIPY 505/515 fluorescent dye, providing *in vivo* visualization of lipid vesicles (Govender et al., 2012). There was a gradual increase in intracellular neutral lipid content accumulated after Hg exposure, marked by the intense green fluorescence in a dose and time dependent manner (Fig. 7A). The measurement of relative fluorescence intensity showed similar trends in lipid accumulation, with exceptionally highest values obtained in cell exposed to 10 μ M Hg after 24 or 72 h (Fig. 7B).

To verify that one of the characteristic responses to Hg was the accumulation of TAGs visualized by BODIPY 505/515 in *C. dorsiventrals*, we analyzed the lipid composition using semi-quantitative thin-layer chromatography (TLC). After biphasic TLC plate elution, we observed the presence of four major components in the lipid extracts (Fig. 8): digalactosylacylglycerol (DGDG) (Band 1), monogalactosylacylglycerol (MGDG) (Band 2), free fatty acids (FFAs) (Band 3) and TAGs (Band 4), identified in comparison with the elution of commercially available standards. The decreases in galactolipids contents (Band 2) were clearly observed after 72 h Hg exposure, a response that matched the patterns previously observed in microalgae subjected to different stress conditions (Li et al., 2022; Wang et al., 2019), and may imply the degradation of thylakoid membrane glycolipids (Yang and Hu, 2020). In addition, TAGs and FFAs (Bands 3 and 4, respectively) bands increased gradually with Hg dose after 24 h treatment, pattern that was maintained after 72 h (Fig. 8). Therefore, the increase in both TAGs and FFAs band intensity confirmed the analytical data obtained by BODIPY 505/515 staining of *C. dorsiventrals* in response to Hg stress, in the same manner that

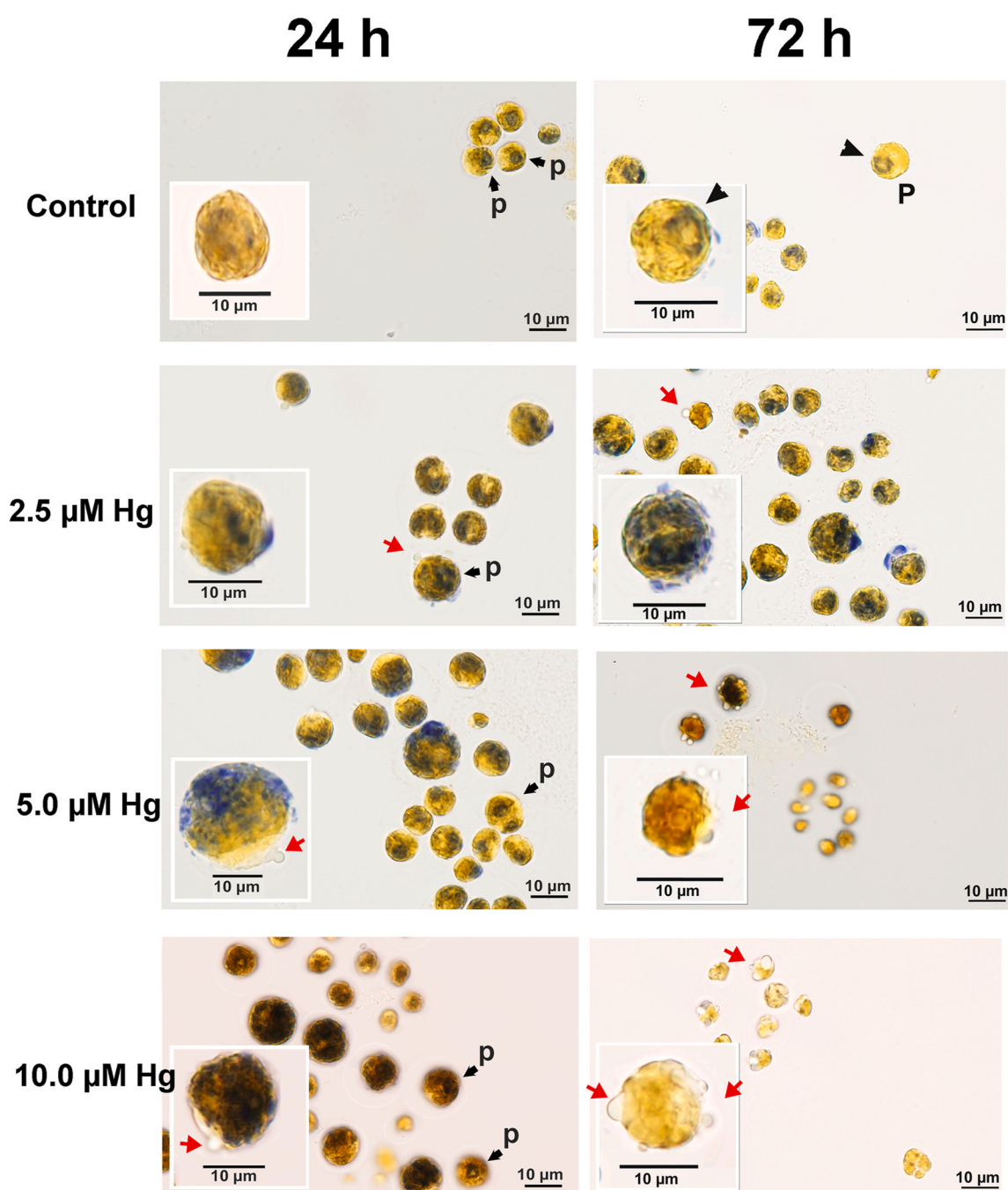


Fig. 6. Effect of short- (24 h) and long-term (72 h) exposure to Hg (0, 2.5, 5 and 10 μM) on starch granules distribution in *C. dorsiventrals*. The dark blue color reveals reactivity of lugol with starch granules. Red arrows: lipid vesicles; Black arrowheads: intact pyrenoid surrounded by starch sheath. (For interpretation of the references to color in this figure legend, the reader is referred to the Web version of this article.)

stronger signal of cytosolic lipid droplets appeared in Hg and Cd treated *Chlamydomonas reinhardtii* (Barón-Sola et al., 2021).

On the other hand, free fatty acid accumulation is not a random phenomenon that occurs in microalgae, because FFAs are converted to fatty acyl-CoA which constitute a crucial precursor for TAGs biosynthesis (Nami et al., 2022). Adverse growth conditions may entrain distinct alteration in the composition of membrane amphipathic lipids (glycerolipids and phospholipids) and the over production of triacyl glycerols (TAGs) (Klok et al., 2014). It is feasible that under stress microalgae divert the biosynthetic glycerolipid metabolism towards the accumulation of TAGs as long-term energy storage to improve cell's survival capacity (Nordin et al., 2020). For example, down-regulation of glycerolipid metabolism occurred in environmental stressors like

polystyrene nanoplastics (PS) and Cd (Cao et al., 2022). Understanding the mechanisms that controls the shift of glycerolipids lipid metabolism towards TAGs accumulation under stress should be the matter of future research, because TAGs can be converted to 'C-neutral' products (bio-diesel) by transesterification (Peccia et al., 2013; Christenson and Sims, 2011). In this sense, *C. dorsiventrals* may constitute a promising feed-stock for future biofuel production that could be coupled with phycor-remediation strategies to clean-up metal polluted marine waters.

4. Conclusions

Our work provides an overview about the physiological behavior and ROS/redox networking of *C. dorsiventrals* cultivated under various

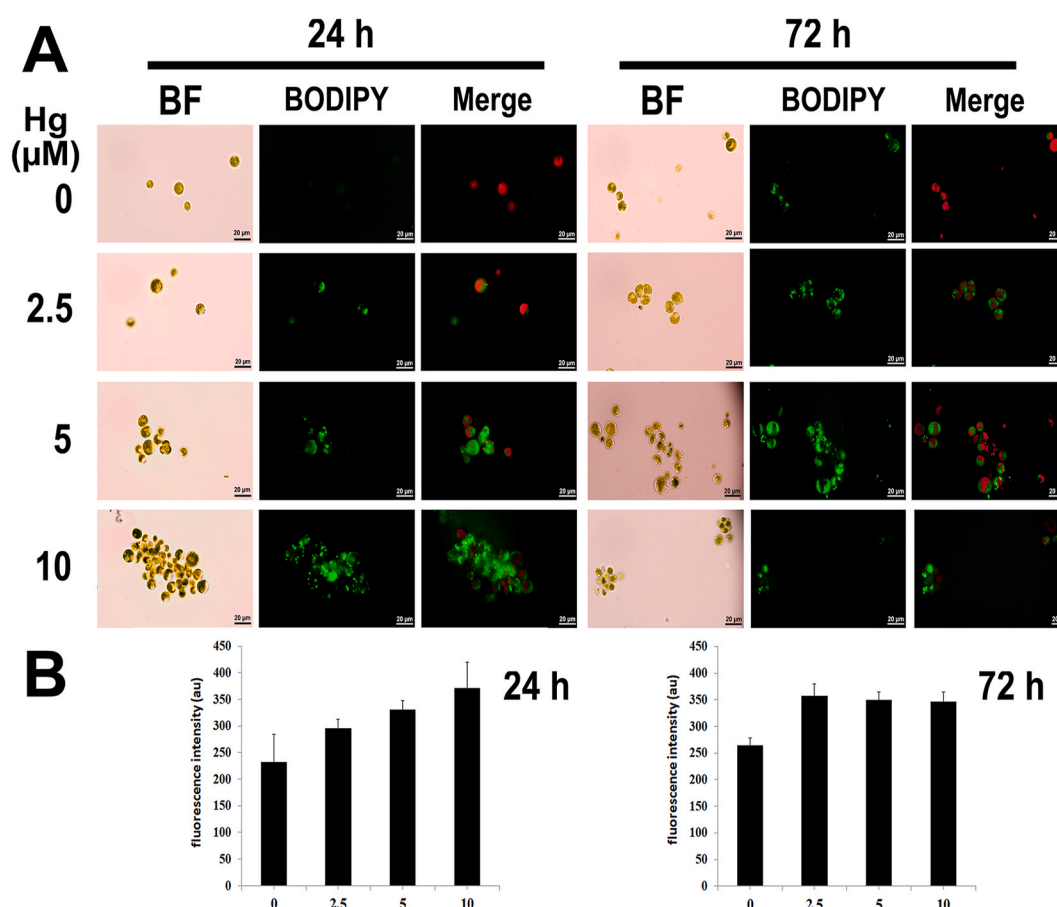


Fig. 7. A) Fluorescence microscopy images of BODIPY 505/515-stained *C. dorsiventrals* cells after exposure to different doses of Hg (0, 2.5, 5 and 10 μM) and exposure times (24 and 72 h). BF: Bright field (BF), BODIPY 505/515 and merged BODIPY 505/515 and chlorophyll autofluorescence images were obtained using fluorescence microscopy. Scale bar = 20 μm . B) BODIPY 505/515 fluorescence intensity (AU) of *C. dorsiventrals*. Error bars represent S.D. of three independent experiment.

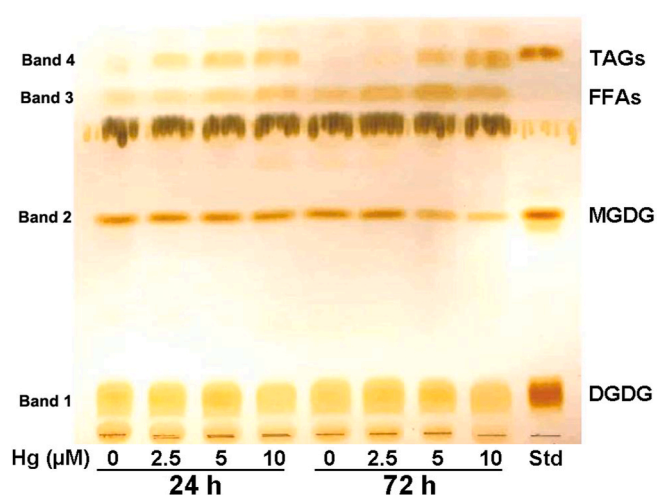


Fig. 8. Thin layer chromatography (TLC) analysis of extracted lipids from *C. dorsiventrals* cultivated at different Hg concentrations (0, 2.5, 5 and 10 μM) for 24 and 72 h. DGDG: digalactosyl-diacylglycerol; MGDG: monogalactosyl-diacylglycerol; TAGs: triacyl glycerides; FFAs: free fatty acids.

concentrations of Hg for short- and long-term exposure times. Mercury accumulation in *C. dorsiventrals* exerted strong changes in biochemical and metabolic fingerprints that could be used as biomarkers of metal stress. The strain showed a greatest potential for neutral lipid

accumulation on expenditure of starch and protein content under unfavorable cultivation conditions, suggesting its applicability for green fuel production and industrial applications. Further studies could be aimed to track the central carbon metabolism networking using isotopically labelled carbon sources, such as [^{13}C]bicarbonate.

Authorship contributions

Jihen Thabet: Conceptualization, methodology, research, data curation, and writing; *Jihen Elleuch*: Methodology, research, supervision, revision of manuscript; *Slim Abdelkafi*: Methodology, supervision, review and editing of manuscript; *Flor Martinez*: Methodology, review and editing of manuscript; *Luis E Hernández*: Methodology, supervision, funding, editing and submission of manuscript; *Imen Fendri*: Methodology, supervision, review and editing of manuscript.

Declaration of competing interest

The authors declare that they have no known competing financial interests or personal relationships that could have appeared to influence the work reported in this paper.

Data availability

No data was used for the research described in the article.

Acknowledgments

This work was supported by grant from the Tunisian Ministry of Higher Education and Scientific Research. This work was also funded by the Spanish Ministry of Science and Technology (AEI) (projects AGL2014-53771-R and AGL2017-87591-R).

Appendix A. Supplementary data

Supplementary data to this article can be found online at <https://doi.org/10.1016/j.chemosphere.2023.139391>.

References

- Ajitha, V., Sreevidya, C.P., Sarasan, M., Park, J.C., Mohandas, A., Singh, I.S.B., Puthumana, J., Lee, J.S., 2021. Effects of zinc and mercury on ROS-mediated oxidative stress-induced physiological impairments and antioxidant responses in the microalgae *Chlorella vulgaris*. *Environ. Sci. Pollut. Res.* 28, 32475–32492. <https://doi.org/10.1007/s11356-021-12950-6>.
- Andrade, L.M., Tito, C.A., Mascarenhas, C., Lima, F.A., Dias, M., Andrade, C.J., Mendes, M.A., Nascimento, C.A.O., 2021. *Chlorella vulgaris* phytoremediation at low Cu²⁺ contents: proteomic profiling of microalgal metabolism related to fatty acids and CO₂ fixation. *Chemosphere* 284. <https://doi.org/10.1016/j.chemosphere.2021.131272>.
- Anjum, N.A., Sharma, P., Gill, S.S., Hasanuzzaman, M., Khan, E.A., Kachhap, K., Mohamed, A.A., Thangavel, P., Devi, G.D., Vasudhevan, P., Sofo, A., Khan, N.A., Misra, A.N., Lukatkin, A.S., Singh, H.P., Pereira, E., Tuteja, N., 2016. Catalase and ascorbate peroxidase—representative H₂O₂-detoxifying heme enzymes in plants. *Environ. Sci. Pollut. Res.* 239, 19002–19029. <https://doi.org/10.1007/s11356-016-7309-6>.
- Annabi-Trabelsi, N., Guermazi, W., Karam, Q., Ali, M., Uddin, S., Leignel, V., Ayadi, H., 2021. Concentrations of trace metals in phytoplankton and zooplankton in the Gulf of Gabès, Tunisia. *Mar. Pollut. Bull.* 168, 112392. <https://doi.org/10.1016/j.marpolbul.2021.112392>.
- Aravind, M.K., Vignesh, N.S., Gayathri, S., Anjitha, N., Athira, K.M., Gunaseelan, S., Arunkumar, M., Sanjaykumar, A., Karthikumar, S., Ganesh Moorthy, I.M., Ashokkumar, B., Pugazhendhi, A., Varalakshmi, P., 2023. Review on rewiring of microalgal strategies for the heavy metal remediation - a metal specific logistics and tactics. *Chemosphere* 313, 137310. <https://doi.org/10.1016/j.chemosphere.2022.137310>.
- Aydi, A., Ghannem, S., Nasri, A., Hessine, R., Mezni, A., 2022. Evaluation of heavy metals contamination and pollution indices levels in surface sediments of the Bizerte coastal line, Tunisia. *Mar. Pollut. Bull.* 184, 114171. <https://doi.org/10.1016/j.marpolbul.2022.114171>.
- Barón-Sola, A., Toledo-Basantes, M., Arana-Gandía, M., Martínez, F., Ortega-Villasante, C., Đučić, T., Yousef, I., Hernández, L.E., 2021. Synchrotron Radiation-Fourier Transformed Infrared microspectroscopy (μSR-FTIR) reveals multiple metabolism alterations in microalgae induced by cadmium and mercury. *J. Hazard Mater.* 419. <https://doi.org/10.1016/j.jhazmat.2021.126502>.
- Bartolomé, M.C., Cortés, A.A., Sánchez-Fortún, A., Garnica-Romo, M.G., Sánchez-Carrillo, S., Sánchez-Fortún, S., 2016. Morphological and physiological changes exhibited by a Cd-resistant *Dictyosphaerium chlorelloides* strain and its cadmium removal capacity. *Int. J. Phytoremediation* 18, 1171–1177. <https://doi.org/10.1080/15226514.2016.1189400>.
- Ben Amor, F., Elleuch, F., Ben Hilma, H., Garnier, M., Saint-Jean, B., Barkallah, M., Pichon, C., Abdelkafi, S., Fendri, I., 2017. Proteomic analysis of the chlorophyta *Dunaliella* new strain AL-1 revealed global changes of metabolism during high carotenoid production. *Mar. Drugs* 15, 1–16. <https://doi.org/10.3390/md15090293>.
- Ben Amor, R., Jerbi, H., Abidi, M., Gueddari, M., 2020. Assessment of trace metal contamination, total organic carbon and nutrient accumulation in surface sediments of Monastir Bay (Eastern Tunisia, Mediterranean Sea). *Reg. Stu. Marine Sci.* 34, 101089. <https://doi.org/10.1016/j.rsmas.2020.101089>.
- Ben Mna, H., Helali, M.A., Oueslati, W., Amri, S., Aleya, L., 2021. Spatial distribution, contamination assessment and potential ecological risk of some trace metals in the surface sediments of the Gulf of Tunis, North Tunisia. *Mar. Pollut. Bull.* 170, 112608. <https://doi.org/10.1016/j.marpolbul.2021.112608>.
- Buege, J.A., Aust, S.D., 1978. Biomembranes - Part C: biological oxidations. *Methods Enzymol.* 52, 302–310. <http://www.sciencedirect.com/science/article/pii/S0076687978520326>.
- Cao, J., Liao, Y., Yang, W., Jiang, X., Li, M., 2022. Enhanced microalgal toxicity due to polystyrene nanoplastics and cadmium co-exposure: from the perspective of physiological and metabolomic profiles. *J. Hazard Mater.* 427, 127937. <https://doi.org/10.1016/j.jhazmat.2021.127937>.
- Cardol, P., Forti, G., Finazzi, G., 2011. Regulation of electron transport in microalgae. *Biochim. Biophys. Acta, Bioenerg.* 1807, 912–918. <https://doi.org/10.1016/j.bbabo.2010.12.004>.
- Carrasco-Gil, S., Ortega-Villasante, C., Sobrino-Plata, J., Barón-Sola, A., Millán, R., Hernandez, L.E., 2023. Attenuation of mercury phytotoxicity with a high nutritional level of nitrate in alfalfa plants grown hydroponically. *Plant Stress* 7, 100131. <https://doi.org/10.1016/j.stress.2023.100131>.
- Chankova, S.G., Dimova, E.G., Mitrovska, Z., Miteva, D., Mokerova, D.V., Yonova, P.A., Yurina, N.P., 2014. Antioxidant and HSP70B responses in *Chlamydomonas reinhardtii* genotypes with different resistance to oxidative stress. *Ecotoxicol. Environ. Saf.* 101, 131–137. <https://doi.org/10.1016/j.ecoenv.2013.11.015>.
- Charles, E.D., Muhamadali, H., Goodacre, R., Pittman, J.K., 2019. Biochemical signatures of acclimation by *Chlamydomonas reinhardtii* to different ionic stresses. *Algal Res* 37, 83–91. <https://doi.org/10.1016/j.algal.2018.11.006>.
- Cherif, F., Ben Hmid, R., Frikha, I., Omar, T., Choura, M., 2020. Assessment of heavy metal contamination in the subsurface sediment of the southern coastal zone of Sfax, Tunisia. *J. Coast Conserv.* 24, 1–8. <https://doi.org/10.1007/s11852-020-00771-7>.
- Christenson, L., Sims, R., 2011. Production and harvesting of microalgae for wastewater treatment, biofuels, and bioproducts. *Biotechnol. Adv.* 29, 686–702. <https://doi.org/10.1016/j.biotechadv.2011.05.015>.
- Choudhary, M., Jetley, U.K., Khan, M.A., Zutshi, S., Fatma, T., 2007. Effect of heavy metal stress on proline, malondialdehyde, and superoxide dismutase activity in the cyanobacterium *Spirulina platensis*-S5. *Ecotoxicol. Environ. Saf.* 66, 204–209.
- Coulombier, N., Jauffrais, T., Lebouvier, N., 2021. Antioxidant compounds from microalgae: a review. *Mar. Drugs* 19. <https://doi.org/10.3390/md19100549>.
- Danouche, M., El Ghatchouli, N., Arroussi, H., 2022. Overview of the management of heavy metals toxicity by microalgae. *J. Appl. Phycol.* 34, 475–488. <https://doi.org/10.1007/s10811-021-02668-w>.
- Elbaz, A., Wei, Y.Y., Meng, Q., Zheng, Q., Yang, Z.M., 2010. Mercury-induced oxidative stress and impact on antioxidant enzymes in *Chlamydomonas reinhardtii*. *Ecotoxicology* 19, 1285–1293. <https://doi.org/10.1007/s10646-010-0514-z>.
- Elleuch, J., Ben Amor, F., Chaaben, Z., Frikha, F., Michaud, P., Fendri, I., Abdelkafi, S., 2021a. Zinc biosorption by *Dunaliella* sp. AL-1: mechanism and effects on cell metabolism. *Sci. Total Environ.* 773. <https://doi.org/10.1016/j.scitotenv.2021.145024>.
- Elleuch, J., Hmani, R., Drira, M., Michaud, P., Fendri, I., Abdelkafi, S., 2021b. Potential of three local marine microalgae from Tunisian coasts for cadmium, lead and chromium removals. *Sci. Total Environ.* 799. <https://doi.org/10.1016/j.scitotenv.2021.149464>.
- Elleuch, J., Jaoua, S., Ginibre, C., Chandre, F., Tounsi, S., Zghal, R.Z., 2016a. Toxin stability improvement and toxicity increase against dipteran and lepidopteran larvae of *Bacillus thuringiensis* crystal protein Cry2Aa. *Pest Manag. Sci.* 72, 2240–2246. <https://doi.org/10.1002/ps.4261>.
- Elleuch, J., Jaoua, S., Tounsi, S., Zghal, R.Z., 2016b. Cry1Ac toxicity enhancement towards lepidopteran pest *Ephestia kuehniella* through its protection against excessive proteolysis. *Toxicon* 120, 42–48. <https://doi.org/10.1016/j.toxicon.2016.07.014>.
- Ghosh, S., Othmani, A., Malloum, A., Ke Christ, O., Onyeaka, H., Alkafaas, S.S., Nnaji, N. D., Bornman, C., Al-Sharif, Z.T., Ahmadi, S., Dehghani, M.H., Mubarak, N.M., Tyagi, I., Karri, R.R., Koduru, J.R., Suhas, 2022. Removal of mercury from industrial effluents by adsorption and advanced oxidation processes: a comprehensive review. *J. Mol. Liquids* 367, 120491. <https://doi.org/10.1016/j.molliq.2022.120491>.
- Gill, S.S., Tuteja, N., 2010. Reactive oxygen species and antioxidant machinery in abiotic stress tolerance in crop plants. *Plant Physiol. Biochem.* 48, 909–930. <https://doi.org/10.1016/j.plaphy.2010.08.016>.
- Govender, T., Ramanna, L., Rawat, I., Bux, F., 2012. BODIPY staining, an alternative to the Nile Red fluorescence method for the evaluation of intracellular lipids in microalgae. *Bioresour. Technol.* 114, 507–511. <https://doi.org/10.1016/j.biortech.2012.03.024>.
- Grajek, H., Rydzynski, D., Piotrowicz-Cieslak, A., Herman, A., Maciejczyk, M., Wiecezorek, Z., 2020. Cadmium ion-chlorophyll interaction – examination of spectral properties and structure of the cadmium-chlorophyll complex and their relevance to photosynthesis inhibition. *Chemosphere* 261. <https://doi.org/10.1016/j.chemosphere.2020.127434>.
- Hamed, S.M., Hassan, S.H., Selim, S., Kumar, A., Khalaf, S.M.H., Wadaan, M.A.M., Hozzein, W.N., AbdElgawad, H., 2019. Physiological and biochemical responses to aluminum-induced oxidative stress in two cyanobacterial species. *Environ. Pollut.* 251, 961–969. <https://doi.org/10.1016/j.envpol.2019.05.036>.
- Hamed, S.M., Okla, M.K., Al-Saadi, L.S., Hozzein, W.N., Mohamed, H.S., Selim, S., AbdElgawad, H., 2022. Evaluation of the phytoremediation potential of microalgae for cadmium removal: comprehensive analysis on toxicity, detoxification and antioxidants modulation. *J. Hazard Mater.* 427, 128177. <https://doi.org/10.1016/j.jhazmat.2021.128177>.
- Hamed, S.M., Zinta, G., Klöck, G., Asard, H., Selim, S., AbdElgawad, H., 2017. Zinc-induced differential oxidative stress and antioxidant responses in *Chlorella sorokiniana* and *Scenedesmus acuminatus*. *Ecotoxicol. Environ. Saf.* 140, 256–263. <https://doi.org/10.1016/j.ecoenv.2017.02.055>.
- Hartl, F.U., 1996. Molecular chaperones in cellular protein folding. *Nature* 381, 571–580. <https://doi.org/10.1038/381571a0>.
- Hazlina, A.Z., Devanathan, L., Fatimah, H., 2019. Morphological changes and DNA damage in *Chlorella vulgaris* (UMT-M1) induced by Hg²⁺. *Malays. Appl. Biol.* 48, 27–33.
- Huang, Y., Qin, M., Lai, J., Liang, J., Luo, X., Li, C., 2023. Assessing OBT formation and enrichment: ROS signaling is involved in the radiation hormesis induced by tritium exposure in algae. *J. Hazard Mater.* 443, 130159. <https://doi.org/10.1016/j.jhazmat.2022.130159>.
- Jebara, A., Turco, V. Lo, Faggio, C., Licata, P., Nava, V., Potorti, A.G., Crupi, R., Mansour, H.B., Bella, G. Di, 2021. Monitoring of environmental hg occurrence in tunisian coastal areas. *Int. J. Environ. Res. Publ. Health* 18. <https://doi.org/10.3390/ijerph18105202>.
- Kajikawa, M., Fukuzawa, H., 2020. Algal autophagy is necessary for the regulation of carbon metabolism under nutrient deficiency. *Front. Plant Sci.* 11, 1–6. <https://doi.org/10.3389/fpls.2020.00036>.

- Kato, Y., Ho, S.H., Vavricka, C.J., Chang, J.S., Hasunuma, T., Kondo, A., 2017. Evolutionary engineering of salt-resistant *Chlamydomonas* sp. strains reveals salinity stress-activated starch-to-lipid biosynthesis switching. *Bioresour. Technol.* 245, 1484–1490. <https://doi.org/10.1016/j.biortech.2017.06.035>.
- Klok, A.J., Lamers, P.P., Martens, D.E., Draaisma, R.B., Wijffels, R.H., 2014. Edible oils from microalgae: insights in TAG accumulation. *Trends Biotechnol.* 32, 521–528. <https://doi.org/10.1016/j.tibtech.2014.07.004>.
- Kováčik, J., Babula, P., Peterková, V., Hedbavny, J., 2017. Long-term impact of cadmium shows little damage in *Scenedesmus acutiformis* cultures. *Algal Res.* 25, 184–190. <https://doi.org/10.1016/j.algalres.2017.06.003>.
- Kumar, K.S., Dahms, H.U., Lee, J.S., Kim, H.C., Lee, W.C., Shin, K.H., 2014. Algal photosynthetic responses to toxic metals and herbicides assessed by chlorophyll a fluorescence. *Ecotoxicol. Environ. Saf.* 104, 51–71. <https://doi.org/10.1016/j.ecoenv.2014.01.042>.
- Le Faucheur, S., Campbell, P.G., Fortin, C., Slaveykova, V.I., 2014. Interactions between mercury and phytoplankton: speciation, bioavailability, and internal handling. *Environ. Toxicol. Chem.* 33, 1211–1224. <https://doi.org/10.1002/etc.2424>.
- León-Vaz, A., Romero, L.C., Gotor, C., León, R., Vigar, J., 2021. Effect of cadmium in the microalga *Chlorella sorokiniana*: a proteomic study. *Ecotoxicol. Environ. Saf.* 207, 111301. <https://doi.org/10.1016/j.ecoenv.2020.111301>.
- Leong, Y.K., Chang, J.S., 2020. Bioremediation of heavy metals using microalgae: recent advances and mechanisms. *Bioresour. Technol.* 303, 122886. <https://doi.org/10.1016/j.biortech.2020.122886>.
- Li, B., Stuart, D.D., Shanta, P.V., Pike, C.D., Cheng, Q., 2022. Probing herbicide toxicity to algae (*Selenastrum capricornutum*) by lipid profiling with machine learning and microchip/MALDI-TOF mass spectrometry. *Chem. Res. Toxicol.* 35, 606–615. <https://doi.org/10.1021/acs.chemrestox.1c00397>.
- Li, T., Gargouri, M., Feng, J., Park, J.J., Gao, D., Miao, C., Dong, T., Gang, D.R., Chen, S., 2015. Regulation of starch and lipid accumulation in a microalga *Chlorella sorokiniana*. *Bioresour. Technol.* 180, 250–257. <https://doi.org/10.1016/j.biortech.2015.01.005>.
- Li, Y., Han, D., Yoon, K., Zhu, S., Sommerfeld, M., Hu, Q., 2013. Molecular and Cellular Mechanisms for Lipid Synthesis and Accumulation in Microalgae: Biotechnological Implications, second ed. Handbook of Microalgal Culture: Applied Physiology and Biotechnology, pp. 545–565. <https://doi.org/10.1002/9781118567166.ch28>.
- Liu, C., Willmund, F., Golecki, J.R., Cacace, S., Heß, B., Markert, C., Schroda, M., 2007. The chloroplast HSP70B-CDJ2-CGE1 chaperones catalyze assembly and disassembly of VIP1 oligomers in *Chlamydomonas*. *Plant J.* 50, 265–277. <https://doi.org/10.1111/j.1365-3113.2007.03047.x>.
- Liu, M., Liu, Y., Zhang, L., Qiu, F., 2022. NADPH oxidase contributes to the production of reactive oxygen species in *Chlorella pyrenoidosa*. *Biotechnol. Lett.* 0123456789. <https://doi.org/10.1007/s10529-022-03330-2>.
- Liu, N., Zhang, H., Zhao, J., Xu, Y., Ge, F., 2020. Mechanisms of cetyltrimethyl ammonium chloride-induced toxicity to photosystem II oxygen evolution complex of *Chlorella vulgaris* F1068. *J. Hazard Mater.* 383, 121063. <https://doi.org/10.1016/j.jhazmat.2019.121063>.
- Liyanage, L.M.M., Lakmal, W.G.M., Athukorala, S.N.P., Jayasundera, K.B., 2020. Application of live *Chlorococcum aquaticum* biomass for the removal of Pb(II) from aqueous solutions. *J. Appl. Phycol.* 32, 4069–4080. <https://doi.org/10.1007/s10811-020-02242-w>.
- Machado, M.D., Lopes, A.R., Soares, E.V., 2015. Responses of the alga *Pseudokirchneriella subcapitata* to long-term exposure to metal stress. *J. Hazard Mater.* 296, 82–92. <https://doi.org/10.1016/j.jhazmat.2015.04.022>.
- Maldonado, J., de los Rios, A., Esteve, I., Ascaso, C., Puyen, Z.M., Brambilla, C., Solé, A., 2010. Sequestration and in vivo effect of lead on DE2009 microalga, using high-resolution microscopic techniques. *J. Hazard Mater.* 183, 44–50. <https://doi.org/10.1016/j.jhazmat.2010.06.085>.
- Merhaby, D., Rabodonirina, S., Net, S., Ouddane, B., Halwani, J., 2019. Overview of sediments pollution by PAHs and PCBs in mediterranean basin: transport, fate, occurrence, and distribution. *Mar. Pollut. Bull.* 149, 110646. <https://doi.org/10.1016/j.marpolbul.2019.110646>.
- Mohamed, B., Elleuch, J., Drira, M., Esteban, M.A., Michaud, P., Abdelkafi, S., Fendri, I., 2021. Characterization and biotechnological potential of two native marine microalgae isolated from the tunisian coast. *Appl. Sci.* 11. <https://doi.org/10.3390/app11115295>.
- Morlon, L., Fortin, C., Floriani, M., Adam, C., Garnier-Laplace, J., Boudou, A., 2005. Toxicity of selenite in the unicellular green alga *Chlamydomonas reinhardtii*: comparison between effects at the population and sub-cellular level. *Aquat. Toxicol.* (N. Y.) 73, 65–78. <https://doi.org/10.1016/j.aquatox.2005.02.007>.
- Mosbahi, N., Serbaji, M.M., Pezy, J.P., Neifar, L., Dauvin, J.C., 2019. Response of benthic macrofauna to multiple anthropogenic pressures in the shallow coastal zone south of Sfax (Tunisia, central Mediterranean Sea). *Environ. Pollut.* 253, 474–487. <https://doi.org/10.1016/j.envpol.2019.06.080>.
- Nami, F., Ferraz, M.J., Bakkum, T., Aerts, J.M.F.G., Pandit, A., 2022. Real-time NMR recording of fermentation and lipid metabolism processes in live microalgae cells. *Angew. Chem.* 61, 1–6. <https://doi.org/10.1002/anie.202117521>.
- Nordin, N., Yusof, N., Maeda, T., Mustapha, N.A., Mohd Yusoff, M.Z., Raja Khairuddin, R. F., 2020. Mechanism of carbon partitioning towards starch and triacylglycerol in *Chlorella vulgaris* under nitrogen stress through whole-transcriptome analysis. *Biomass Bioenergy* 138, 105600. <https://doi.org/10.1016/j.biombioe.2020.105600>.
- Nowicka, B., 2022. Heavy metal-induced stress in eukaryotic algae—mechanisms of heavy metal toxicity and tolerance with particular emphasis on oxidative stress in exposed cells and the role of antioxidant response. *Environ. Sci. Pollut. Res.* 29, 16860–16911. <https://doi.org/10.1007/s11356-021-18419-w>.
- Nesci, S., Trombetti, F., Pirini, M., Ventrella, V., Pagliarini, A., 2016. Mercury and protein thiols: stimulation of mitochondrial F₁F₀-ATPase and inhibition of respiration. *Chem. Biol. Interact.* 260, 42–49. <https://doi.org/10.1016/j.cbi.2016.10.018>.
- Ortega-Villasante, C., Burén, S., Blázquez-Castro, A., Barón-Sola, Á., Hernández, L.E., 2018. Fluorescent *in vivo* imaging of reactive oxygen species and redox potential in plants. *Free Radical Biol. Med.* 122, 202–220. <https://doi.org/10.1016/j.freeradbiomed.2018.04.005>.
- Ortega-Villasante, C., Barón-Sola, Á., Toledo-Basantes, M., Martínez, F., Hernández, L.E., 2021. Characterization of oxidative lipidomics and autophagy induction in *Chlamydomonas reinhardtii* under abiotic stress. *Methods Mol. Biol.* 2202, 71–80. https://doi.org/10.1007/978-1-0716-0896-8_6.
- Paliwal, C., Mitra, M., Bhayani, K., Bharadwaj, S.V., Ghosh, T., Dubey, S., Mishra, S., 2017. Abiotic stresses as tools for metabolites in microalgae. *Bioresour. Technol.* 244, 1216–1226. <https://doi.org/10.1016/j.biortech.2017.05.058>.
- Pandey, A., Pathak, V.V., Kothari, R., Black, P.N., Tyagi, V.V., 2019. Experimental studies on zeta potential of flocculants for harvesting of algae. *J. Environ. Manag.* 231, 562–569. <https://doi.org/10.1016/j.jenvman.2018.09.096>.
- Peccia, J., Haznedaroglu, B., Gutierrez, J., Zimmerman, J.B., 2013. Nitrogen supply is an important driver of sustainable microalgae biofuel production. *Trends Biotechnol.* 31, 134–138. <https://doi.org/10.1016/j.tibtech.2013.01.010>.
- Penen, F., Isaure, M.P., Dobritzsch, D., Castillo-Michel, H., Gontier, E., Le Coustumer, P., Malherbe, J., Schaumlöffel, D., 2020. Pyrenoid sequestration of cadmium impairs carbon dioxide fixation in a microalga. *Plant Cell Environ.* 43, 479–495. <https://doi.org/10.1111/pce.13674>.
- Peng, Y., Deng, A., Gong, X., Li, X., Zhang, Y., 2017. Coupling process study of lipid production and mercury bioremediation by biomimetic mineralized microalgae. *Bioresour. Technol.* 243, 628–633. <https://doi.org/10.1016/j.biortech.2017.06.165>.
- Pérez-Pérez, M.E., Couso, I., Heredia-Martínez, L.G., Crespo, J.L., 2017. Monitoring autophagy in the model green microalga *Chlamydomonas reinhardtii*. *Cells* 6, 1–11. <https://doi.org/10.3390/cells6040036>.
- Pérez-Pérez, M.E., Lemaire, S.D., Crespo, J.L., 2021. The ATG4 protease integrates redox and stress signals to regulate autophagy. *J. Exp. Bot.* 72, 3340–3351. <https://doi.org/10.1093/jxb/erab063>.
- Qiu, C., Wang, W., Zhang, Y., Zhou, G.J., Bi, Y., 2022. Response of antioxidant enzyme activities of the green microalga *Chlorococcum* sp. AZHB to Cu²⁺ and Cd²⁺ stress. *Sustainability* 14. <https://doi.org/10.3390/su141610320>.
- Razzak, S.A., Lucky, R.A., Hossain, M.M., deLasa, H., 2022. Valorization of microalgae biomass to biofuel production: a review. *Energy Nexus* 7, 100139. <https://doi.org/10.1016/j.nexus.2022.100139>.
- Rebai, N., Mosbahi, N., Dauvin, J.-C., Neifar, L., 2022. Ecological risk assessment of heavy metals and environmental quality of tunisian harbours. *J. Mar. Sci. Eng.* 10, 1625. <https://doi.org/10.3390/jmse10111625>.
- Renuka, N., Sood, A., Prasanna, R., Ahluwalia, A.S., 2015. Phycoremediation of wastewaters: a synergistic approach using microalgae for bioremediation and biomass generation. *Int. J. Environ. Sci. Tech.* 12, 1443–1460. <https://doi.org/10.1007/s13762-014-0700-2>.
- Rezayian, M., Niknam, V., Ebrahimpzadeh, H., 2019. Oxidative damage and antioxidative system in algae. *Toxicol Rep* 6, 1309–1313. <https://doi.org/10.1016/j.toxrep.2019.10.001>.
- Samson, G., Popovic, R., 1990. Inhibitory effects of mercury on photosystem II photochemistry in *Dunaliella tertiolecta* under *in vivo* conditions. *J. Photochem. Photobiol. B, Biol.* 5, 303–310. [https://doi.org/10.1016/1011-1344\(90\)85046-Y](https://doi.org/10.1016/1011-1344(90)85046-Y).
- Sanchez-Wandellmer, J., Ktistakis, N.T., Reggiori, F., 2015. ERES: sites for autophagosome biogenesis and maturation? *J. Cell Sci.* 128, 185–192. <https://doi.org/10.1242/jcs.158758>.
- Seoane, M., Esperanza, M., Cid, Á., 2017. Cytotoxic effects of the proton pump inhibitor omeprazole on the non-target marine microalga *Tetraselmis suecica*. *Aquat. Toxicol.* (N. Y.) 191, 62–72. <https://doi.org/10.1016/j.aquatox.2017.08.001>.
- Shao, Y., Wang, Y., Zhu, D., Xiong, X., Tian, Z., Balakin, A.V., Shkurinov, A.P., Xu, D., Wu, Y., Peng, Y., Zhu, Y., 2022. Measuring heavy metal ions in water using nature existed microalgae as medium based on terahertz technology. *J. Hazard Mater.* 435, 129028. <https://doi.org/10.1016/j.jhazmat.2022.129028>.
- Sharma, S.K., Goloubinoff, P., Christen, P., 2008. Heavy metal ions are potent inhibitors of protein folding. *Biochem. Biophys. Res. Commun.* 372, 341–345. <https://doi.org/10.1016/j.bbrc.2008.05.052>.
- Shi, Z., Guo, M., Du, H., Yang, K., Liu, X., Xu, H., 2023. Investigation of cytotoxic cadmium in aquatic green algae by synchrotron radiation-based Fourier transform infrared spectroscopy: role of dissolved organic matter. *Sci. Total Environ.* 870. <https://doi.org/10.1016/j.scitotenv.2023.161870>.
- Sobrinho-Plata, J., Meysen, D., Cuypers, A., Escobar, C., Hernández, L.E., 2014. Glutathione is a key antioxidant metabolite to cope with mercury and cadmium stress. *Plant Soil* 377, 369–381. <https://doi.org/10.1007/s11104-013-2006-4>.
- Song, X., Liu, B.F., Kong, F., Ren, N.Q., Ren, H.Y., 2022. Overview on stress-induced strategies for enhanced microalgae lipid production: application, mechanisms and challenges. *Resour. Conserv. Recycl.* 183, 106355. <https://doi.org/10.1016/j.resconrec.2022.106355>.
- Tripathi, S., Arora, N., Pruthi, V., Poluri, K.M., 2021. Elucidating the bioremediation mechanism of *Scenedesmus* sp. *IITRIND2* under cadmium stress. *Chemosphere* 283, 131196. <https://doi.org/10.1016/j.chemosphere.2021.131196>.
- Tripathi, S., Poluri, K.M., 2021. Heavy metal detoxification mechanisms by microalgae: insights from transcriptomics analysis. *Environ. Pollut.* 285, 117443. <https://doi.org/10.1016/j.envpol.2021.117443>.
- Upadhyay, A.K., Singh, L., Singh, R., Singh, D.P., Saxena, G., 2022. Bioaccumulation and toxicity of as in the alga *Chlorococcum* sp.: prospects for as bioremediation. *Bull. Environ. Contam. Toxicol.* 108, 500–506. <https://doi.org/10.1007/s00128-020-02964-0>.

- Vinson, J.A., Hao, Y., Su, X., Zubik, L., 1998. Phenol antioxidant quantity and quality in foods: vegetables. *J. Agric. Food Chem.* 46, 3630–3634. <https://doi.org/10.1021/jf980295o>.
- Wang, J., Chen, R., Fan, L., Cui, L., Zhang, Y., Cheng, J., Wu, X., Zeng, W., Tian, Q., Shen, L., 2021. Construction of fungi-microalgae symbiotic system and adsorption study of heavy metal ions. *Sep. Purif. Technol.* 268, 118689. <https://doi.org/10.1016/j.seppur.2021.118689>.
- Wang, L., Huang, X., Lim, D.J., Laserna, A.K.C., Li, S.F.Y., 2019. Uptake and toxic effects of triphenyl phosphate on freshwater microalgae *Chlorella vulgaris* and *Scenedesmus obliquus*: insights from untargeted metabolomics. *Sci. Total Environ.* 650, 1239–1249. <https://doi.org/10.1016/j.scitotenv.2018.09.024>.
- Wang, S., Duo, J., Wufuer, R., Li, W., Pan, X., 2022. The binding ability of mercury (Hg) to photosystem I and II explained the difference in its toxicity on the two photosystems of *Chlorella pyrenoidosa*. *Toxics* 10, 455. <https://doi.org/10.3390/toxics10080455>.
- Wang, X., Li, Y., Wei, S., Pan, L., Miao, J., Lin, Y., Wu, J., 2021. Toxicity evaluation of butyl acrylate on the photosynthetic pigments, chlorophyll fluorescence parameters, and oxygen evolution activity of *Phaeodactylum tricornutum* and *Platymonas subcordiformis*. *Environ. Sci. Pollut. Res.* 28, 60954–60967. <https://doi.org/10.1007/s11356-021-15070-3>.
- Weis, J.S., 2015. *Marine Pollution: what Everyone Needs to Know*. Oxford University Press.
- Xiao, X., Li, W., Jin, M., Zhang, L., Qin, L., Geng, W., 2023. Responses and tolerance mechanisms of microalgae to heavy metal stress: a review. *Mar. Environ. Res.* 183, 105805. <https://doi.org/10.1016/j.marenvres.2022.105805>.
- Yan, Z., Xu, L., Zhang, W., Yang, G., Zhao, Z., Wang, Y., Li, X., 2021. Comparative toxic effects of microplastics and nanoplastics on *Chlamydomonas reinhardtii*: growth inhibition, oxidative stress, and cell morphology. *J. Water Proc. Eng.* 43, 102291. <https://doi.org/10.1016/j.jwpe.2021.102291>.
- Yang, H., Hu, C., 2020. Regulation and remodeling of intermediate metabolite and membrane lipid during NaCl-induced stress in freshwater microalga *Micractinium sp.* XJ-2 for biofuel production. *Biotechnol. Bioeng.* 117, 3727–3738. <https://doi.org/10.1002/bit.27528>.
- Yang, J.S., Cao, J., Xing, G.L., Yuan, H.L., 2015. Lipid production combined with biosorption and bioaccumulation of cadmium, copper, manganese and zinc by oleaginous microalgae *Chlorella minutissima* UTEX2341. *Bioresour. Technol.* 175, 537–544. <https://doi.org/10.1016/j.biortech.2014.10.124>.
- Yong, W.K., Sim, K.S., Poong, S.W., Wei, D., Phang, S.M., Lim, P.E., 2021. Interactive effects of warming and copper toxicity on a tropical freshwater green microalga *Chloromonas augustae* (Chlorophyceae). *J. Appl. Phycol.* 33, 67–77. <https://doi.org/10.1007/s10811-020-02087-3>.
- Zada, S., Raza, S., Khan, S., Iqbal, A., Kai, Z., Ahmad, A., Ullah, M., Kakar, M., Fu, P., Dong, H., Xueji, Z., 2022. Microalgal and cyanobacterial strains used for the bio sorption of copper ions from soil and wastewater and their relative study. *J. Ind. Engin. Chem.* 105, 463–472. <https://doi.org/10.1016/j.jiec.2021.10.003>.
- Zamani-Ahmadmarmoodi, R., Malekabadi, M.B., Rahimi, R., Johari, S.A., 2020. Aquatic pollution caused by mercury, lead, and cadmium affects cell growth and pigment content of marine microalga. *Nannochloropsis oculata*. *Environmental Monit. Ass.* 192. <https://doi.org/10.1007/s10661-020-8222-5>.
- Zamora-Ledezma, C., Negrete-Bolagay, D., Figueroa, F., Zamora-Ledezma, E., Ni, M., Alexis, F., Guerrero, V.H., 2021. Heavy metal water pollution: a fresh look about hazards, novel and conventional remediation methods. *Environ. Tech. Inn.* 22, 101504. <https://doi.org/10.1016/j.eti.2021.101504>.
- Zaynab, M., Al-Yahyai, R., Ameen, A., Sharif, Y., Ali, L., Fatima, M., Khan, K.A., Li, S., 2022. Health and environmental effects of heavy metals. *J. King Saud Univ. Sci.* 34, 101653. <https://doi.org/10.1016/j.jksus.2021.101653>.
- Zhang, F., Zhang, H., Wang, G., Xu, L., Shen, Z., 2009. Cadmium-induced accumulation of hydrogen peroxide in the leaf apoplast of *Phaseolus aureus* and *Vicia sativa* and the roles of different antioxidant enzymes. *J. Hazard Mater.* 168, 76–84. <https://doi.org/10.1016/j.jhazmat.2009.02.002>.
- Zhang, X.P., Glaser, E., 2002. Interaction of plant mitochondrial and chloroplast signal peptides with the Hsp70 molecular chaperone. *Trends Plant Sci.* 7, 14–21. [https://doi.org/10.1016/S1360-1385\(01\)02180-X](https://doi.org/10.1016/S1360-1385(01)02180-X).
- Zharova, D.A., Ivanova, A.N., Drozdova, I.V., Belyaeva, A.I., Boldina, O.N., Voitikhovskaja, O.V., Tyutereva, E.V., 2022. Role of autophagy in *Haematococcus lacustris* cell growth under salinity. *Plants* 11, 1–19. <https://doi.org/10.3390/plants11020197>.
- Zheng, Y., Huang, Y., Xia, A., Qian, F., Wei, C., 2019. A rapid inoculation method for microalgae biofilm cultivation based on microalgae-microalgae co-flocculation and zeta-potential adjustment. *Bioresour. Technol.* 278, 272–278. <https://doi.org/10.1016/j.biortech.2019.01.083>.
- Zrelli, S., Amairia, S., Chaabouni, M., Oueslati, W., Chine, O., Nachi Mkaouer, A., Cheikhbouii, A., Ghorbel, R., Zrelli, M., 2021. Contamination of fishery products with mercury, cadmium, and lead in Tunisia: level's estimation and human health risk assessment. *Biol. Trace Elem. Res.* 199, 721–731. <https://doi.org/10.1007/s12011-020-02179-8>.